A unified surface tension model for multi-component salt, organic, and surfactant solutions

Supplemental Material

Judith Kleinheins ,*[a] Claudia Marcolli,[a] Cari S. Dutcher,[b] Nadia Shardt[c]

[a] *Institute for Atmospheric and Climate Science, ETH Zürich, Universitätstrasse 16, 8092 Zürich, Switzerland. E-mail: judith.kleinheins@env.ethz.ch*
[b] *Department of Mechanical Engineering and Department of Chemical Engineering and Materials Science, University of Minnesota, Twin Cities, Minneapolis, MN 55455, USA*
[c] *Department of Chemical Engineering, Norwegian University of Science and Technology (NTNU), 7491 Trondheim, Norway*

Contents

S1 Relationship between the Sigmoid model and the Eberhart model

The Sigmoid model was derived by Kleinheins *et al.*[1] as

$$\sigma^{\text{Sig}} = \sigma_1 - (\sigma_1 - \sigma_2)\left(10^{pd}+1\right)\frac{x_2^d}{10^{pd}+x_2^d}. \tag{S1}$$

When plotting σ^{Sig} on a logarithmic x_2-axis, the function has its inflection point at a mole fraction of $x_2 = 10^p$. The parameter d is related to the distance of the CMC from the inflection point (more details see in Kleinheins *et al.*[1]). If $d = 1$ is chosen, the Sigmoid model simplifies to a function that is mathematically equivalent to the Eberhart model since:

$$\sigma^{\text{Sig}}(d=1) = \sigma_1 - (\sigma_1 - \sigma_2)(10^p+1)\frac{x_2}{10^p+x_2} \tag{S2}$$

$$\sigma^{\text{Sig}}(d=1) = \frac{\sigma_1(10^p+x_2)}{10^p+x_2} - \frac{(\sigma_1-\sigma_2)(10^p+1)x_2}{10^p+x_2} \tag{S3}$$

$$\sigma^{\text{Sig}}(d=1) = \frac{10^p\sigma_1 + x_2\sigma_1 - x_2(\sigma_1-\sigma_2)10^p - x_2(\sigma_1-\sigma_2)}{10^p+x_2} \tag{S4}$$

$$\sigma^{\text{Sig}}(d=1) = \frac{10^p(\sigma_1 - x_2(\sigma_1-\sigma_2)) + x_2\sigma_2}{10^p+x_2}. \tag{S5}$$

Under the assumption of $10^p = 1/(S_{12}-1)$, we get

$$\sigma^{\text{Sig}}(d=1) = \frac{\frac{1}{S_{12}-1}(\sigma_1 - x_2(\sigma_1-\sigma_2)) + x_2\sigma_2}{\frac{1}{S_{12}-1}+x_2} \tag{S6}$$

which can be rearranged to

$$\sigma^{\text{Sig}}(d=1) = \frac{\sigma_1(1-x_2) + \sigma_2 S_{12}x_2}{(1-x_2) + S_{12}x_2} = \sigma^{\text{Eb}}. \tag{S7}$$

Thus, the Sigmoid model reduces to the Eberhart model, with $d = 1$ and $10^p = 1/(S_{12}-1)$.

To verify if $1/(S_{12}-1)$ is also related to the inflection point of the Eberhart model, we derive the inflection point of the Eberhart model on a logarithmic x_2-axis as follows. The Eberhart model can be written as

$$\sigma^{\text{Eb}} = \frac{x_2(S_{12}\sigma_2-\sigma_1)+\sigma_1}{x_2(S_{12}-1)+1}. \tag{S8}$$

Since the inflection point is defined for a logarithmic x_2-scale, we introduce a new variable y defined as

$$y = \log_{10}x_2, \tag{S9}$$

which leads to

$$\sigma^{\text{Eb}} = \frac{10^y(S_{12}\sigma_2-\sigma_1)+\sigma_1}{10^y(S_{12}-1)+1}. \tag{S10}$$

The first derivative of Equation S10 is

$$\frac{\partial\sigma}{\partial y} = \ln(10)S_{12}(\sigma_2-\sigma_1)\frac{10^y}{(10^y(S_{12}-1)+1)^2}, \tag{S11}$$

and the second derivative gives

$$\frac{\partial^2\sigma}{\partial y^2} = \ln(10)^2 S_{12}(\sigma_2-\sigma_1)\frac{-10^y(10^y(S_{12}-1)-1)}{(10^y(S_{12}-1)+1)^3}. \tag{S12}$$

The inflection point $\hat{p}$ of the Eberhart model is given by

$$\frac{\partial^2 \sigma}{\partial y^2}(y = \hat{p}) = 0 \tag{S13}$$

leading to

$$\ln(10)^2 S_{12} (\sigma_2 - \sigma_1) \frac{-10^{\hat{p}} \left(10^{\hat{p}} (S_{12} - 1) - 1\right)}{\left(10^{\hat{p}} (S_{12} - 1) + 1\right)^3} = 0 \tag{S14}$$

$$10^{\hat{p}} (S_{12} - 1) - 1 = 0 \tag{S15}$$

and finally

$$10^{\hat{p}} = \frac{1}{S_{12} - 1} = 10^p, \tag{S16}$$

showing that the inflection point of the Eberhart model is given by $1/(S_{12} - 1)$ and equal to the inflection point of the Sigmoid model.

S2   Derivation of the multi-component Eberhart model

Through analogy to the Connors-Wright model[2,3] and the Chunxi model[4], the multi-component Eberhart model was derived. The relationship between these models and their main assumptions in the derivation are summarized in Fig. S1 and described in the following.
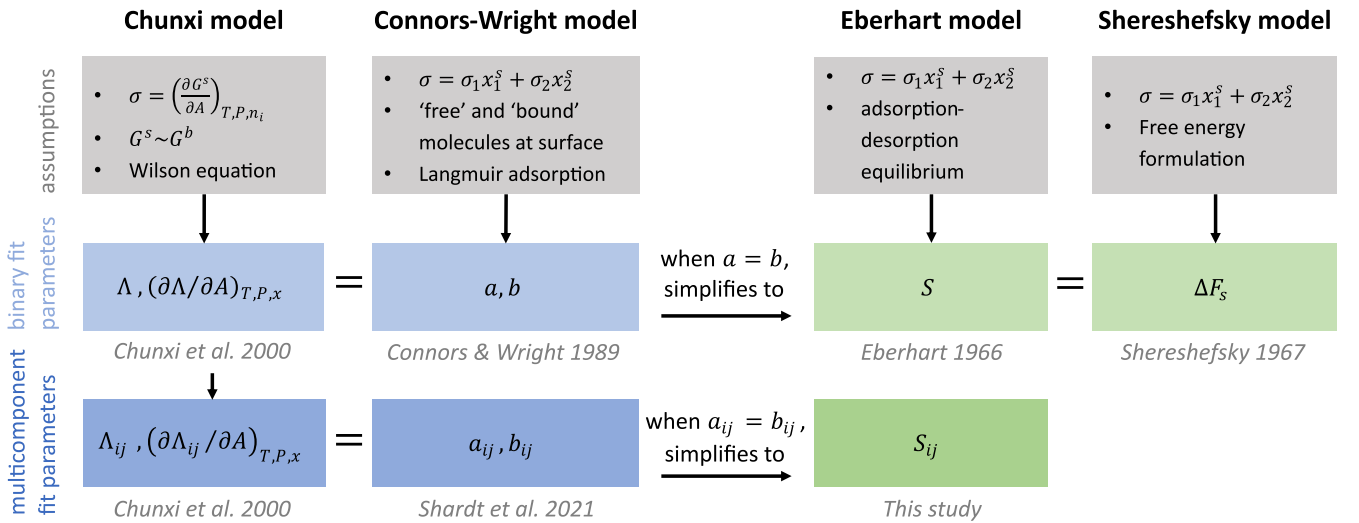

Figure S1: Overview of the four models discussed in Section S2 (columns) and an illustration of their relationships. The first row summarizes some basic assumptions in the derivation of the binary models. The second and third row show the fit parameters and the reference to the first publication of the binary and multi-component versions of the models, respectively. Equal signs indicate that the two respective models are mathematically equivalent.

In 2000, a multi-component model was derived by Chunxi *et al.*[4] by assuming that the Gibbs free energy in the surface G^s is proportional to the one in the bulk G^b. The surface tension was defined as the change of G^s with area A at constant temperature T, pressure P and mole number n_i:

$$\sigma = \left(\frac{\partial G^s}{\partial A}\right)_{T,P,n_i}. \tag{S17}$$

For the molar excess Gibbs energy, the Wilson equation[5] was assumed to be valid. The resulting model is written as

$$\sigma = \sum_{i=1}^{n} x_i \sigma_i - RT \sum_{i=1}^{n} \left(\frac{x_i}{\sum_{j=1}^{n} x_j \Lambda_{ij}} \sum_{j=1}^{n} x_j \left(\frac{\partial \Lambda_{ij}}{\partial A}\right)_{T,P,x}\right) \tag{S18}$$

where Λ_{ij} and $\left(\frac{\partial \Lambda_{ij}}{\partial A}\right)_{T,P,x}$ are fit parameters for the binary surface tension of substances i and j, with $\Lambda_{ii} = 1$, and $\left(\frac{\partial \Lambda_{ii}}{\partial A}\right)_{T,P,x} = 0$. Analyzing the equations given in Chunxi *et al.*[4] for a binary system, the following conversion rules can be derived:

$$\Lambda_{ij} = 1/\Lambda ji, \qquad \left(\frac{\partial \Lambda_{ij}}{\partial A}\right)_{T,P,x} = -\left(\Lambda_{ij}\right)^2 \left(\frac{\partial \Lambda_{ji}}{\partial A}\right)_{T,P,x}. \tag{S19}$$

By comparison of the binary surface tension equations of the Chunxi and Connors-Wright models, it has been found that the models are mathematically equivalent[6], with

$$a_{ij} = 1 - \Lambda_{ji}, \qquad b_{ij} = -\frac{RT}{\sigma_j - \sigma_i} \left(\frac{\partial \Lambda_{ji}}{\partial A}\right)_{T,P,x} \left[1 - \frac{1}{\Lambda_{ji}}\right], \tag{S20}$$

where a_{ij} and b_{ij} replace the original fit parameters a and b of the Connors-Wright model[2]. By combination of Equations S18, S19, and S20, a multi-component Connors-Wright model has been derived[3], which, following the naming conventions in this paper, reads as

$$\sigma = \sum_{i=1}^{n} \sigma_i x_i + \sum_{i=1}^{n} \left(\frac{x_i}{\sum_{j=1}^{n} x_j \left(1 - a_{ji}\right)} \sum_{j=1}^{n} x_j \frac{b_{ji}}{a_{ji}} \left(a_{ji} - 1\right) \left(\sigma_j - \sigma_i\right) \right). \tag{S21}$$

The binary Eberhart model was found to be a simplified version of the binary Connors-Wright model[1]. Setting the two fit parameters a and b in the Connors-Wright model equal, the model reduces to the Eberhart model and its fit parameter S relates to a and b as

$$a = b = 1 - 1/S. \tag{S22}$$

Analogously, by setting a_{ij} equal to b_{ij} in Equation S21, the multi-component Eberhart model (Equation 6 in the main paper) was derived.

The Shereshefsky model is mathematically equivalent to the Eberhart model[1] with $S = \exp\left(\Delta F_s / RT\right)$. As such, a multi-component Shereshefsky model could be formulated as well by simple conversion of the fit parameters.

S3 Experimental surface tension data of multi-component systems

S3.1 Ternary mixtures

Table S1: Experimental surface tension data of **inorganic–inorganic–water** systems in the literature: Sources, components, measurement temperature T, and number of measured data points N_p

No.	Source	Components	T (°C)	N_p
1	Belton[7]	NaCl, KCl, water	25	12
2	Belton[7]	HCl, NaCl, water	25	15
3	Belton[8]	NaCl, HCl, water	25	5
4	Belton[8]	KCl, HCl, water	25	4
5	Boyer *et al.*[9]	NH_4NO_3, $(NH_4)_2SO_4$, water		4
6	Dutcher *et al.*[10]	KNO_3, NH_4Cl, water	18	10
7	Dutcher *et al.*[10]	$NaNO_3$, $(NH_4)_2SO_4$, water	18	9
8	Dutcher *et al.*[10]	NH_4Cl, $(NH_4)_2SO_4$, water	18	10
9	Dutcher *et al.*[10]	HNO_3, KNO_3, water	20-80	244
10	Dutcher *et al.*[10]	KNO_3, NH_4NO_3, water	20-80	143
11	Hyvärinen *et al.*[11]	H_2SO_4, NH_3, water	25	42
12	Martin *et al.*[12]	H_2SO_4, HNO_3, water	20.15	20
13	Martin *et al.*[12]	H_2SO_4, HNO_3, water	20.15	20
14	Matubayasi *et al.*[13]	NaCl, Na_2SO_4, water	15-35	12
15	Matubayasi *et al.*[13]	NaCl, NaI, water	15-35	9
16	Nehma *et al.*[14]	NH_4NO_3, $NaNO_3$, water	25	6

Table S2: Experimental surface tension data of **surfactant–surfactant–water** systems in the literature: Sources, components, measurement temperature T, and number of measured data points N_p

No.	Source	Components	T (°C)	N_p
1	Alam *et al.*[15]	SDS, CTAB, water	25	38
2	Bagheri and Abolhasani[16]	C14PC, TX100, water	25	>180
3	Bagheri and Abolhasani[16]	C16PC, TX100, water	25	>180
4	Das *et al.*[17]	CPC, TTAB, water	29.85	13
5	Das *et al.*[17]	DPC, TTAB, water	29.85	11
6	Das *et al.*[17]	CPC, DPC, water	29.85	8
7	El Haber *et al.*[18]	SDS, CTAC, water	24	41
8	El Haber *et al.*[18]	Triton-X-114, SDS, water	24	73
9	Fainerman *et al.*[19]	SdeS, SDS, water		12
10	Funasaki and Hada[20]	DeMS, De7, water	30	50
11	Jańczuk *et al.*[21]	SDDS, SDS, water	20	72
12	Jańczuk *et al.*[21]	SDDS, TX100, water	20	59
13	Mulqueen and Blankschtein[22]	SDS, C12E6, water	25	28
14	Mulqueen and Blankschtein[22]	SDS, C12Maltoside, water	25	45
15	Mulqueen and Blankschtein[23]	C12Maltoside, C12Betaine, water	25	13
16	Mulqueen and Blankschtein[23]	SDS, C12Betaine, water	25	7
17	Siddiqui and Franses[24]	TritonX100 C12EO5, water	25	33
18	Siddiqui and Franses[24]	SDS, C12E8, water		35
19	Szymczyk *et al.*[25]	CTAB, CPyB, water	20	61
20	Szymczyk and Jańczuk[26]	CTAB, TX100, water	20	55
21	Szymczyk and Jańczuk[27]	TX100, TX165, water	20	64
22	Szymczyk and Jańczuk[28]	CTAB, TX165, water	20	15
23	Szymczyk[29]	Zonyl FSN-100, TX100, water	20	18
24	Szymczyk[29]	Zonyl FSO-100, TX100, water	20	18
25	Szymczyk[29]	Zonyl FSN-100, TX165, water	20	18
26	Szymczyk[29]	Zonyl FSO-100, TX165, water	20	18
27	Szymczyk *et al.*[30]	CTAB, TX-100, water	20	15
28	Taraba and Szymczyk[31]	Zonyl FSN-100, Zonyl FSO-100, water	20	64
29	Tyagi *et al.*[32]	SDS, DDAO, water	25	53
30	Zakharova *et al.*[33]	Brij35, SDS, water	25	60
31	Zhang and Zhao[34]	C8PyBr, C8SNa, water	30	34
32	Zhang and Zhao[34]	C6PyBr, C7FNa, water	30	17
33	Zhang and Zhao[34]	C6PyBr, C10SNa, water	30	11

Table S3: Experimental surface tension data of **organic–organic–water** systems in the literature: Sources, components, measurement temperature T, and number of measured data points N_p

No.	Source	Components	T (°C)	N_p
1	Bartovská *et al.*[35]	MTBE, ethanol, water	25	8
2	Bartovská *et al.*[35]	MTBE, tert-butanol, water	25	10
3	Bartovská *et al.*[35]	MTBE, 1-butanol, water	25	12
4	Bošković *et al.*[36]	ethanol, octanol, water	25	15
5	Costa *et al.*[37]	n-butyl acetate, 1-propanol, water	50	29
6	Dzhambulatov *et al.*[38]	1,4-dioxane, acetone, water	20	10
7	Dzhambulatov *et al.*[38]	glycerol, ethanol, water	20	30
8	El Haber *et al.*[18]	glutaric acid, oxalic acid, water	24	39
9	Enders *et al.*[39]	acetone, toluene, water	15	32
10	Enders *et al.*[39]	acetone, toluene, water	25	32
11	Enders *et al.*[39]	acetone, toluene, water	35	32
12	Enders *et al.*[39]	acetone, toluene, water	45	32
13	Enders *et al.*[39]	acetone, toluene, water	55	31
14	Ernst *et al.*[40]	glycerol, ethanol, water	25	36
15	Fainerman *et al.*[19]	1-heptanol, 1-octanol, water		51
16	Golmaghani-Ebrahimi *et al.*[41]	acetonitrile, methanol, water	25	44
17	Golmaghani-Ebrahimi *et al.*[41]	acetonitrile, ethanol, water	25	45
18	Gómez-Díaz and Navaza[42]	hexamethylenetetramine, ethanol, water	20	22
19	Gómez-Díaz and Navaza[42]	hexamethylenetetramine, ethanol, water	30	22
20	Gómez-Díaz and Navaza[42]	hexamethylenetetramine, ethanol, water	40	22
21	Gómez-Díaz and Navaza[42]	hexamethylenetetramine, ethanol, water	50	22
22	Hey and Kippax[43]	n-pentanol, tert-butanol, water	25	>100
23	Johnson *et al.*[44]	n-butyl acetate, 1-propanol, water	30	43
24	Kharin *et al.*[45]	ethanol, methanol, water	5	28
25	Kharin *et al.*[45]	ethanol, methanol, water	10	28
26	Kharin *et al.*[45]	ethanol, methanol, water	20	28
27	Kharin *et al.*[45]	ethanol, methanol, water	30	28
28	Kharin *et al.*[45]	ethanol, methanol, water	40	28
29	Kharin *et al.*[45]	ethanol, methanol, water	50	28
30	Kharin *et al.*[45]	ethanol, methanol, water	60	28
31	Kijevcanin *et al.*[46]	ethyl butyrate, methanol, water	30	33
32	Kijevcanin *et al.*[47]	ethyl propionate, methanol, water	30	33
33	Lamperski[48]	acetone, propionic acid, water		23
34	Rafati *et al.*[49]	acetonitrile, 2-propanol, water	25	32
35	Rafati *et al.*[50]	acetonitrile, 1,2-ethandiol, water	25	52
36	Santos *et al.*[51]	n-butyl acetate, methanol, water	30	48
37	Santos *et al.*[51]	n-pentyl acetate, methanol, water	30	26

Table S4: Experimental surface tension data of **surfactant–organic–water** systems in the literature: Sources, components, measurement temperature T, and number of measured data points N_p

No.	Source	Components	T (°C)	N_p
1	Beiranvand *et al.*[52]	PEG 300, Triton CG-110, water	20	8
2	Beiranvand *et al.*[52]	PEG 300, DDAB, water	20	9
3	Beiranvand *et al.*[52]	PEG 300, SDS, water	20	8
4	Bielawska *et al.*[53]	CTAB, methanol	19.85	>200
5	Bielawska *et al.*[53]	CTAB, ethanol	19.85	>200
6	Bielawska *et al.*[53]	CTAB, 1-propanol	19.85	>200
7	Bzdek *et al.*[54]	Triton-X-100, glutaric acid, water		27
8	El Haber *et al.*[18]	TritonX100, glutaric acid, water	24	101
9	El Haber *et al.*[18]	TritonX114, glutaric acid, water	24	27
10	El Haber *et al.*[18]	Brij35, glutaric acid, water	24	80
11	El Haber *et al.*[18]	TritonX100, oxalic acid, water	24	63
12	El Haber *et al.*[18]	Brij35, oxalic acid, water	24	49
13	El Haber *et al.*[18]	CTAC, oxalic acid, water	24	56
14	El Haber *et al.*[18]	SDS, oxalic acid, water	24	45
15	Khosharay *et al.*[55]	CTAB, 1-propanol, water	25	46
16	Khosharay *et al.*[55]	CTAB, 2-propanol, water	25	46
17	Khosharay *et al.*[55]	CTAB, 1-butanol, water	25	47
18	Kwaśniewska and Kiewlicz[56]	SDS, ascorbic acid, water	24.35	28
19	Kwaśniewska and Kiewlicz[56]	SDS, 3-O-ethyl ascorbate, water	24.35	33
20	Kwaśniewska and Kiewlicz[56]	SDS, ascorbyl glucoside, water	24.35	25
21	Kwaśniewska and Kiewlicz[57]	CTAB, ascorbic acid, water	25.85	15
22	Kwaśniewska and Kiewlicz[57]	CTAB, 3-O-ethyl ascorbate, water	25.85	17
23	Kwaśniewska and Kiewlicz[57]	CTAB, ascorbyl glucoside, water	25.85	15
24	Wüstneck and Miller[58]	SDS, n-butanol, water		29
25	Wüstneck and Miller[58]	SDS, n-hexanol, water		9
26	Wüstneck and Miller[58]	SDS, n-nonanol, water		23

Table S5: Experimental surface tension data of **surfactant–salt–water** systems in the literature: Sources, components, measurement temperature T, and number of measured data points N_p

No.	Source	Components	T (°C)	N_p
1	Bzdek *et al.*[54]	Triton-X-100, NaCl, water		24
2	Dar *et al.*[59]	C16Br, NaCl, water	25	16
3	Dar *et al.*[59]	C16BzCl, NaCl, water	25	14
4	Dar *et al.*[59]	Brij58, NaCl, water		16
5	El Haber *et al.*[18]	Triton-X-100, NaCl, water	24	37
6	El Haber *et al.*[18]	Triton-X-100, $(NH_4)_2SO_4$, water	24	11
7	El Haber *et al.*[18]	Brij35, $(NH_4)_2SO_4$, water	24	16
8	El Haber *et al.*[18]	Brij35, NaCl, water	24	43
9	Helvaci *et al.*[60]	Rhamnolipid 1, NaCl, water	25	45
10	Helvaci *et al.*[60]	Rhamnolipid 2, NaCl, water	25	45
11	Matijević and Pethica[61]	SDS, NaCl, water	20	50
12	Matijević and Pethica[61]	SDS, NaCl, water	40	40
13	Matijević and Pethica[61]	SDS, NaCl, water	60	43
14	Nakahara *et al.*[62]	CTAB, NaBr, water	25.05	74
15	Nakahara *et al.*[62]	SDS, NaCl, water	25.05	100
16	Para *et al.*[63]	CTAB, KCl, water	21.85	149
17	Para *et al.*[63]	CTAB, KBr, water	21.85	57
18	Para *et al.*[63]	CTAC, KBr, water	21.85	33
19	Para *et al.*[63]	CTAC, KCl, water	21.85	25
20	Qazi *et al.*[64]	CTAB, NaCl, water		>450
21	Qazi *et al.*[64]	Tween 80, NaCl, water		>240
22	Reid *et al.*[65]	CTAC, NaCl, water	19	6
23	Reid *et al.*[65]	sodium oleate, NaCl, water	19	6
24	Soule *et al.*[66]	hexanoic acid, NaCl, water	25	10
25	Soule *et al.*[66]	hexanoic acid, Na_2SO_4, water	25	10

Table S6: Experimental surface tension data of **organic–salt–water** systems in the literature: Sources, components, measurement temperature T, and number of measured data points N_p

No.	Source	Components	T (°C)	N_p
1	Belton[67]	ethyl alcohol, salts(10 different), water	25	1-5
2	Belton[67]	acetic acid, salts(5 different), water	25	1-5
3	Belton[8]	NaCl, sucrose, water	25	21
4	Booth *et al.*[68]	oxalic acid, $(NH_4)_2SO_4$, water	25	7
5	Booth *et al.*[68]	malonic acid, $(NH_4)_2SO_4$, water	25	16
6	Booth *et al.*[68]	succinic acid, $(NH_4)_2SO_4$, water	25	9
7	Booth *et al.*[68]	glutaric acid, $(NH_4)_2SO_4$, water	25	9
8	Booth *et al.*[68]	adipic acid, $(NH_4)_2SO_4$, water	25	3
9	Booth *et al.*[68]	glutaric acid, salts(4 different), water	25	1
10	Boyer *et al.*[9]	NaCl, glutaric acid, water		10
11	Ekström *et al.*[69]	$(NH_4)_2SO_4$/NaCl, mannitol, water		9
12	Ekström *et al.*[69]	$(NH_4)_2SO_4$/NaCl, methylerythritol, water		9
13	Ekström *et al.*[69]	$(NH_4)_2SO_4$/NaCl, methylthreitol, water		9
14	Ekström *et al.*[69]	$(NH_4)_2SO_4$/NaCl, adipic acid, water		6
15	El Haber *et al.*[18]	glutaric acid, NaCl, water	24	36
16	El Haber *et al.*[18]	glutaric acid, $(NH_4)_2SO_4$, water	24	22
17	Frosch *et al.*[70]	$(NH_4)_2SO_4$, oxalic acid, water	room T.	4
18	Frosch *et al.*[70]	$(NH_4)_2SO_4$, succinic acid, water	room T.	6
19	Frosch *et al.*[70]	$(NH_4)_2SO_4$, adipic acid, water	room T.	5
20	Frosch *et al.*[70]	$(NH_4)_2SO_4$, citric acid, water	room T.	6
21	Frosch *et al.*[70]	$(NH_4)_2SO_4$, NRFA, water	room T.	7
22	Frosch *et al.*[70]	$(NH_4)_2SO_4$, cis-pinonic acid, water	room T.	9
23	Hyvärinen *et al.*[71]	sulfuric acid, dimethylamine, water	25	98
24	Kiss *et al.*[72]	humic acid, $(NH_4)_2SO_4$, water	25	19
25	Kiss *et al.*[72]	NRFA/SRFA, $(NH_4)_2SO_4$, water	25	12
26	Lee *et al.*[73]	NaCl, glucose, water	room T.	8
27	Li *et al.*[74]	acetaldehyde, $(NH_4)_2SO_4$, water		13
28	Li *et al.*[74]	formaldehyde, $(NH_4)_2SO_4$, water		13
29	Miles *et al.*[75]	glutaric acid, NaCl, water	room T.	30
30	Nehma *et al.*[14]	$NaNO_3$, propylene glycol, water	25	5
31	Nehma *et al.*[14]	NH_4NO_3, propylene glycol, water	25	5
32	Rublova *et al.*[76]	ethylene glycol, choline chloride, water	25	14
33	Rublova *et al.*[76]	ethylene glycol, choline chloride, water	30	14
34	Rublova *et al.*[76]	ethylene glycol, choline chloride, water	40	14
35	Rublova *et al.*[76]	ethylene glycol, choline chloride, water	50	14
36	Rublova *et al.*[76]	ethylene glycol, choline chloride, water	60	14
37	Rublova *et al.*[76]	ethylene glycol, choline chloride, water	70	14
38	Sahu *et al.*[77]	4-hydroxyacetophenone, NaCl, water	22	12
39	Sareen *et al.*[78]	methylglyoxal, NaCl, water		10
40	Sareen *et al.*[78]	methylglyoxal, $(NH_4)_2SO_4$, water		10
41	Shulman *et al.*[79]	cis-pinonic acid, $(NH_4)_2SO_4$, water	room T.	13
42	Topping *et al.*[80]	$(NH_4)_2SO_4$, pinonic acid, water		7
43	Topping *et al.*[80]	$(NH_4)_2SO_4$, succinic acid, water		5
44	Topping *et al.*[80]	NaCl, oxalic acid, water		4
45	Tuckermann[81]	cis-pinonic acid, NaCl, water	20	45
46	Tuckermann[81]	cis-pinonic acid, $MgCl_2$, water	20	51
47	Tuckermann[81]	cis-pinonic acid, $AlCl_3$, water	20	30
48	Tuckermann[81]	cis-pinonic acid, NH_4Cl, water	20	20
49	Tuckermann[81]	cis-pinonic acid, Na_2SO_4, water	20	16
50	Tuckermann[81]	azelaic acid, NaCl, water	20	7
51	Vanhanen *et al.*[82]	succinic acid, NaCl, water	10.3	10
52	Vanhanen *et al.*[82]	succinic acid, NaCl, water	15.2	11
53	Vanhanen *et al.*[82]	succinic acid, NaCl, water	20.2	14
54	Vanhanen *et al.*[82]	succinic acid, NaCl, water	25.15	16
55	Vanhanen *et al.*[82]	succinic acid, NaCl, water	30.15	16
56	Werner *et al.*[83]	succinic acid, $(NH_4)_2SO_4$, water	10	18

S3.2 Higher order mixtures

Table S7: Experimental surface tension data of higher order mixtures in the literature: Sources, number of components N_c, components, category, temperature T, and number of measured data points N_p. The categories (cat.) refer to the type of solutes: 1: all salts, 2: all organics, 3: all surfactants, 4: organics + salts, 5: surfactants + salts, 6: surfactants + organics

No.	Source	N_c	Components	cat.	T (°C)	N_p
1	Svenningsson et al. [84]	4	levoglucosan, succinic acid, fulvic acid, water	2		5
2	Chen et al. [85]	4	SDS, STS, NaCl, water	3	30-50	13
3	Das et al. [17]	4	CPC, DPC, TTAB, water	3	30	11
4	Jańczuk et al. [21]	4	FC1, FC2, SDDS, water	3	20	16
5	Jańczuk et al. [21]	4	CTAB, TX100, FC1, water	3	20	16
6	Jańczuk et al. [86]	4	CTAB, TX100, FC1, water	3	20	32
7	Jańczuk et al. [86]	4	CTAB, TX100, FC2, water	3	20	32
8	Mulqueen and Blankschtein [23]	4	C12Maltoside, C12Betaine, SDS, water	3	25	10
9	Szymczyk and Jańczuk [28]	4	CTAB, TX100, TX165, water	3	20	>100
10	Szymczyk et al. [30]	4	CTAB, TX-100, TX-114, water	3	20	45
11	Szymczyk et al. [87]	4	CTAB, TX165, FC1, water	3	20	25
12	Szymczyk et al. [87]	4	CTAB, TX165, FC2, water	3	20	25
13	Henning et al. [88]	4	adipic acid, succinic acid, NaCl, water	4	0-34	36
14	Li et al. [74]	4	formaldehyde, methylglyoxal, $(NH_4)_2SO_4$, water	4		3
15	Li et al. [74]	4	acetaldehyde, methylglyoxal, $(NH_4)_2SO_4$, water	4		6
16	Schwier et al. [89]	4	methylglyoxal, glyoxal, $(NH_4)_2SO_4$, water	4		30
17	Schwier et al. [90]	4	acetaldehyde, $(NH_4)_2SO_4$, leucine, water	4		7
18	Schwier et al. [90]	4	glyoxal, $(NH_4)_2SO_4$, serine, water	4		5
19	Schwier et al. [90]	4	methylglyoxal, $(NH_4)_2SO_4$, leucine, water	4		6
20	Schwier et al. [90]	4	methylglyoxal, $(NH_4)_2SO_4$, acetaldehyde, water	4		3
21	Dar et al. [59]	4	CBr, CBzCl, NaCl, water	5	25	>50
22	Dar et al. [59]	4	CBr, Brij58, NaCl, water	5	25	>50
23	Dar et al. [59]	4	CBzCl, Brij58, NaCl, water	5	25	>50
24	Funasaki and Hada [20]	4	dodecylmethylsulfoxid, CTAB, NaBr, water	5	25	39
25	Funasaki and Hada [20]	4	dodecylmethylsulfoxid, CTAB, KBr, water	5	30	22
26	Góralczyk et al. [91]	4	R10PyCl, R5SO3Na, NaCl, water	5	25	30
27	Góralczyk et al. [91]	4	R12PyCl, R5SO3Na, NaCl, water	5	25	30
28	Góralczyk et al. [91]	4	R10PyCl, R7SO3Na, NaCl, water	5	25	26
29	Góralczyk et al. [91]	4	R12PyCl, R7SO3Na, NaCl, water	5	25	21
30	Góralczyk et al. [91]	4	R10PyCl, R5SO3Na, NaBr, water	5	25	11
31	Góralczyk et al. [91]	4	R10PyCl, R5SO3Na, NaI, water	5	25	10
32	Góralczyk et al. [91]	4	R12PyCl, R5SO3Na, NaBr, water	5	25	8
33	Góralczyk et al. [91]	4	R12PyCl, R5SO3Na, NaI, water	5	25	8
34	Góralczyk et al. [91]	4	R10PyCl, R7SO3Na, NaBr, water	5	25	8
35	Góralczyk et al. [91]	4	R10PyCl, R7SO3Na, NaI, water	5	25	8
36	Góralczyk et al. [91]	4	R12PyCl, R7SO3Na, NaBr, water	5	25	8
37	Góralczyk et al. [91]	4	R12PyCl, R7SO3Na, NaI, water	5	25	6
38	Zhang and Zhao [34]	4	C8PyBr, C8SNa, NaBr, water	5	30	30
39	Zhang and Zhao [34]	4	C6PyBr, C7FNa, NaBr, water	5	30	18
40	Zhang and Zhao [34]	4	C6PyBr, C10SNa, NaBr, water	5	30	16
41	Li et al. [74]	5	formaldehyde, acetaldehyde, methylglyoxal, $(NH_4)_2SO_4$, water	4		7
42	Schwier et al. [90]	5	formaldehyde, acetaldehyde, methylglyoxal, $(NH_4)_2SO_4$, water	4		3
43	Svenningsson et al. [84]	5	$(NH_4)_2SO_4$, levoglucosan, succinic acid, fulvic acid, water	4		7
44	Svenningsson et al. [84]	5	$(NH_4)_2SO_4$, NaCl, succinic acid, fulvic acid, water	4		6
45	Dar et al. [59]	5	CBr, CBzCl, Brij58, NaCl, water	5	25	>50
46	Tuckermann and Cammenga [92]	6	humic acid, azelaic acid, 3-hydroxybutanoic acid, 3-hydroxybenzoic acid, levoglucosan, water	2	20	10
47	Svenningsson et al. [84]	6	NH_4NO_3, $(NH_4)_2SO_4$, levoglucosan, succinic acid, fulvic acid, water	4		6
48	Tuckermann and Cammenga [92]	7	humic acid, pinonic acid, azelaic acid, 3-hydroxybutanoic acid, 3-hydroxybenzoic acid, levoglucosan, water	2	20	10
49	Schwier et al. [90]	8	$(NH_4)_2SO_4$, acetaldehyde, formaldehyde, glyoxal, methylglyoxal, oxalic acid, succinic acid, water	4		6

S4 Comparison of the Eberhart and Connors-Wright models

In previous studies, the Connors-Wright model has been found to be slightly more accurate than the Eberhart or Shereshefsky model for the fitting of the surface tension of aqueous solutions of soluble small organic substances[1,6]. Here, we tested if the Connors-Wright model also performs better in reproducing the ternary data of the two systems shown in Section 4.1 in the main paper.

S4.1 Water–acetonitrile–1,2-ethanediol

Table S8: Fit parameters of the Connors-Wright model[2] for water (1) + acetonitrile (2) + 1,2-ethanediol (3) at 25 °C[50]

	a_{12}	b_{12}	a_{13}	b_{13}	a_{23}	b_{23}
Fitted value	0.95278	0.96922	0.83014	0.77771	-0.88234	-1.6155
95 % confidence interval	± 0.0077168	± 0.042106	± 0.005978	± 0.011714	± 0.69770	± 0.34344

In Fig. S2, the performance of the Eberhart model and the Connors-Wright model for the ternary data of this system is shown as well as a direct comparison of the predicted values of the two models (right plot). It can be seen that the Connors-Wright model has a slightly better performance (RMSE = $1.0\,\mathrm{mN\,m^{-1}}$) than the Eberhart model (RMSE = $1.14\,\mathrm{mN\,m^{-1}}$), but the differences are very small (maximum difference of the modelled surface tension between the two models $\Delta\sigma_{\mathrm{max}} = 0.67\,\mathrm{mN\,m^{-1}}$). The differences in the prediction of the surface tension of ternary mixtures originate partly from the fit quality of the water-free mixture acetonitrile (2) + 1,2-ethanediol (3) which is shown in Fig. S3. The slightly improved fit quality arises from the presence of an extra fitting parameter in the Connors–Wright model.
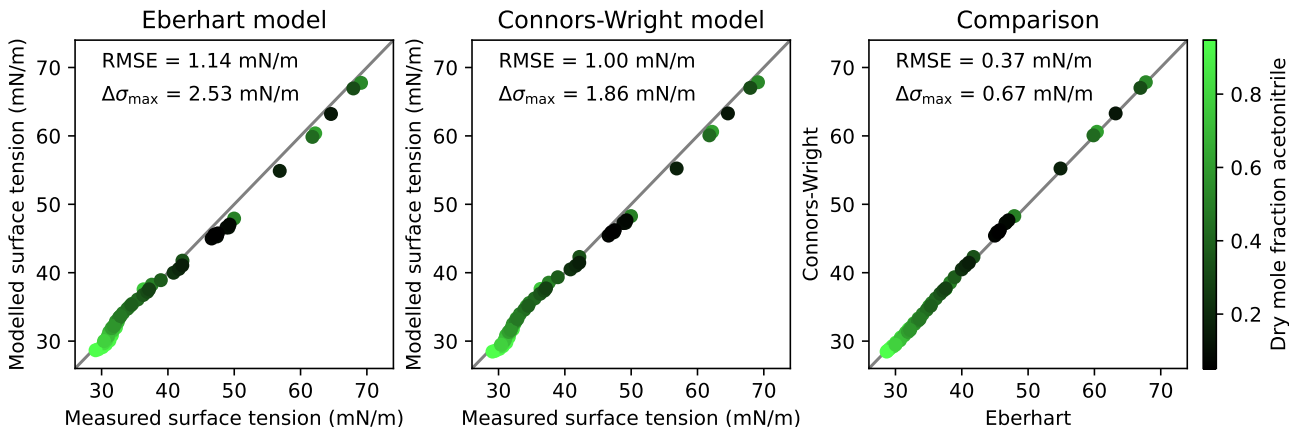

Figure S2: Ternary system water (1) + acetonitrile (2) + 1,2-ethanediol (3): Comparison of the performance of the Eberhart model and the Connors-Wright model.
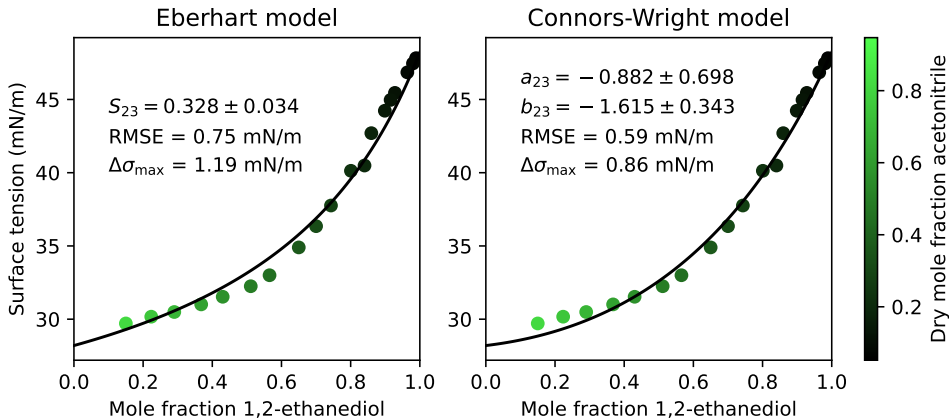

Figure S3: Binary system acetonitrile (2) + 1,2-ethanediol (3)

S4.2 Water–n-butyl acetate–methanol

Table S9: Fit parameters of the Connors-Wright model[2] for water (1) + n-butyl acetate (2) + methanol (3) at 25 °C[51]

	a_{12}	b_{12}	a_{13}	b_{13}	a_{23}	b_{23}
Fitted value	0.9980	0.9584	0.90565	0.751048	-0.07133	-1.00715
95 % confidence interval	± 0.00099	± 0.0121597	± 0.0043085	± 0.01076	± 0.3465	± 0.1756

In Fig. S4, the performance of the Eberhart model and the Connors-Wright model for the ternary data of this system is shown as well as a direct comparison of the predicted values of the two models (right plot). It can be seen that the Connors-Wright model has a better performance (RMSE = $0.33\,\mathrm{mN\,m^{-1}}$) than the Eberhart model (RMSE = $0.41\,\mathrm{mN\,m^{-1}}$) with a maximum difference of the modelled surface tension between the two models $\Delta\sigma_{\mathrm{max}}$ = $0.4\,\mathrm{mN\,m^{-1}}$). The differences in the prediction of the surface tension of ternary mixtures originates partly in differences in the fit of the binary mixture water (1) + methanol (3) which is shown in Fig. S5.
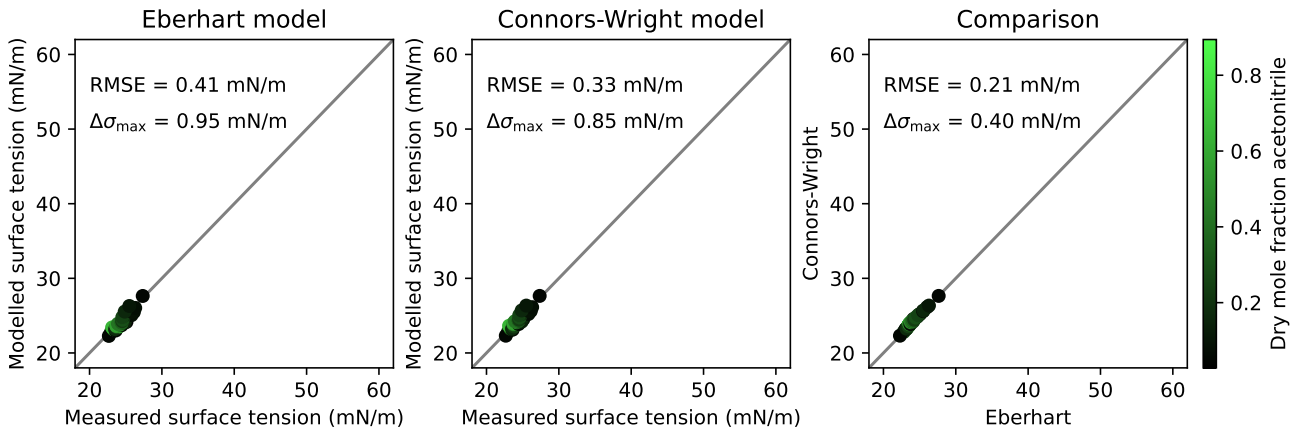

Figure S4: Ternary system water (1) + n-butyl acetate (2) + 1,2-ethanediol (3): Comparison of the performance of the Eberhart model and the Connors-Wright model.
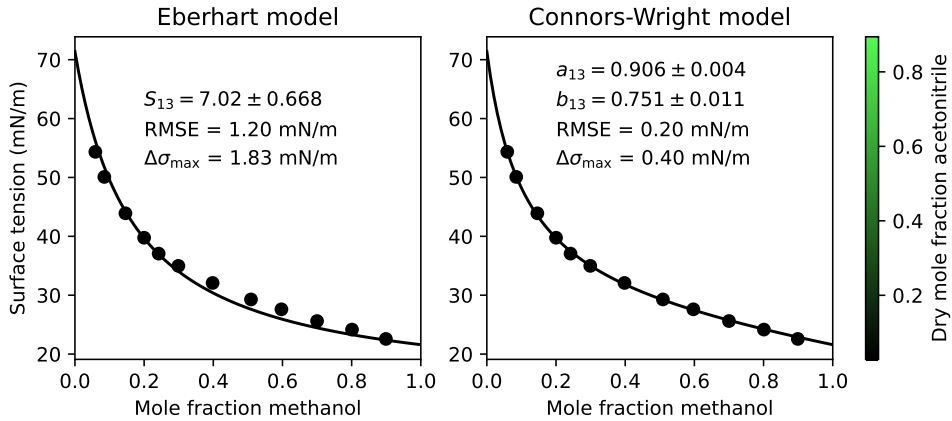

Figure S5: Binary system water (1) + methanol (3)

S5 Binary Eberhart model fits
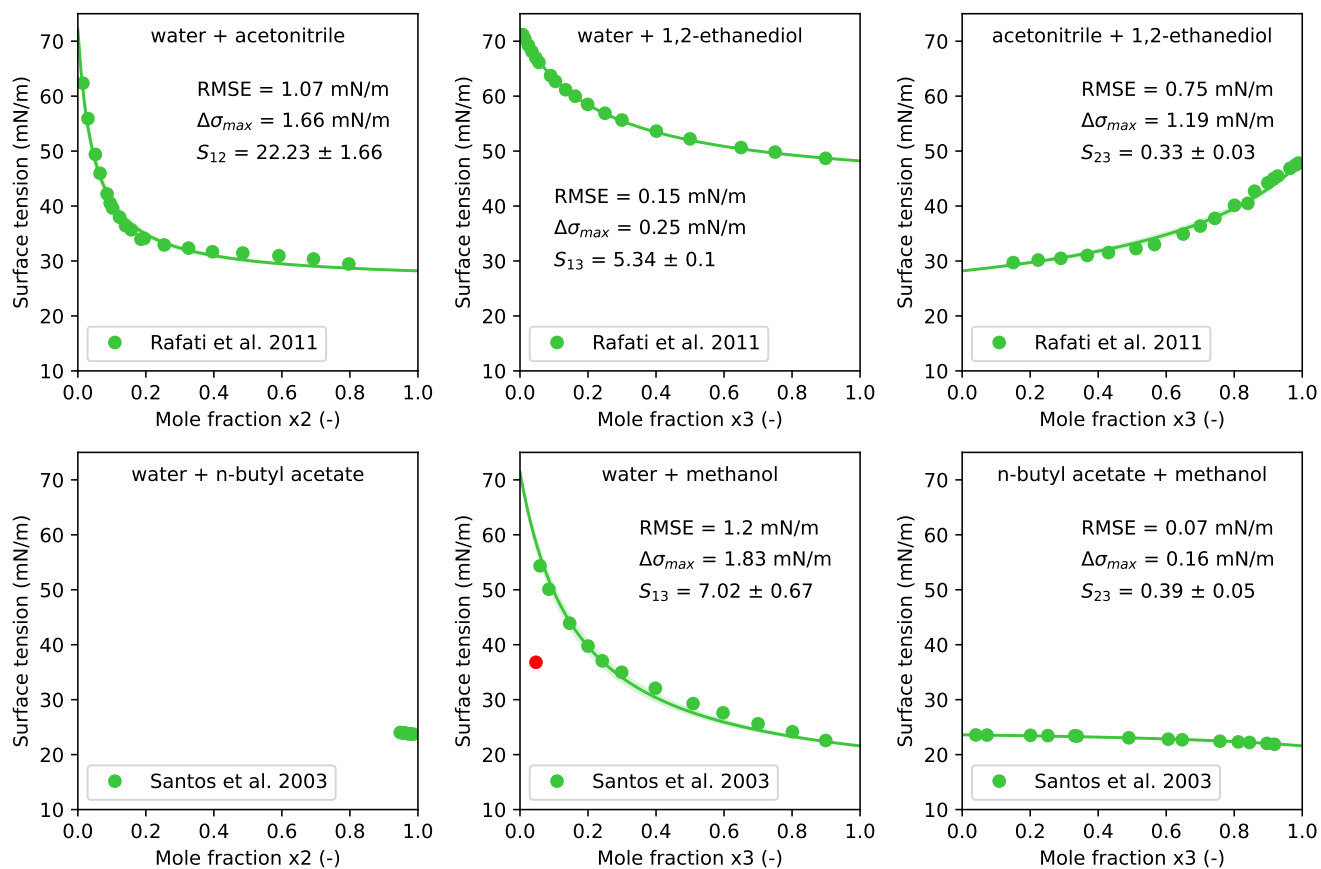
S5.1 Binary fits for water–organic–organic systems

Figure S6: Binary fits with the Eberhart model for the ternary systems water (1) + acetonitrile (2) + 1,2-ethanediol (3) from Rafati *et al.*[50] and water (1) + n-butyl acetate (2) + methanol (3) from Santos *et al.*[51]. Light green shading shows the 95% confidence interval of the fit. No fit was made for the binary system water + n-butyl acetate due to the little coverage of the data space by the measurements because of the miscibility gap of this system. The red data point in the water + methanol plot was considered an outlier and therefore not included for the fitting.

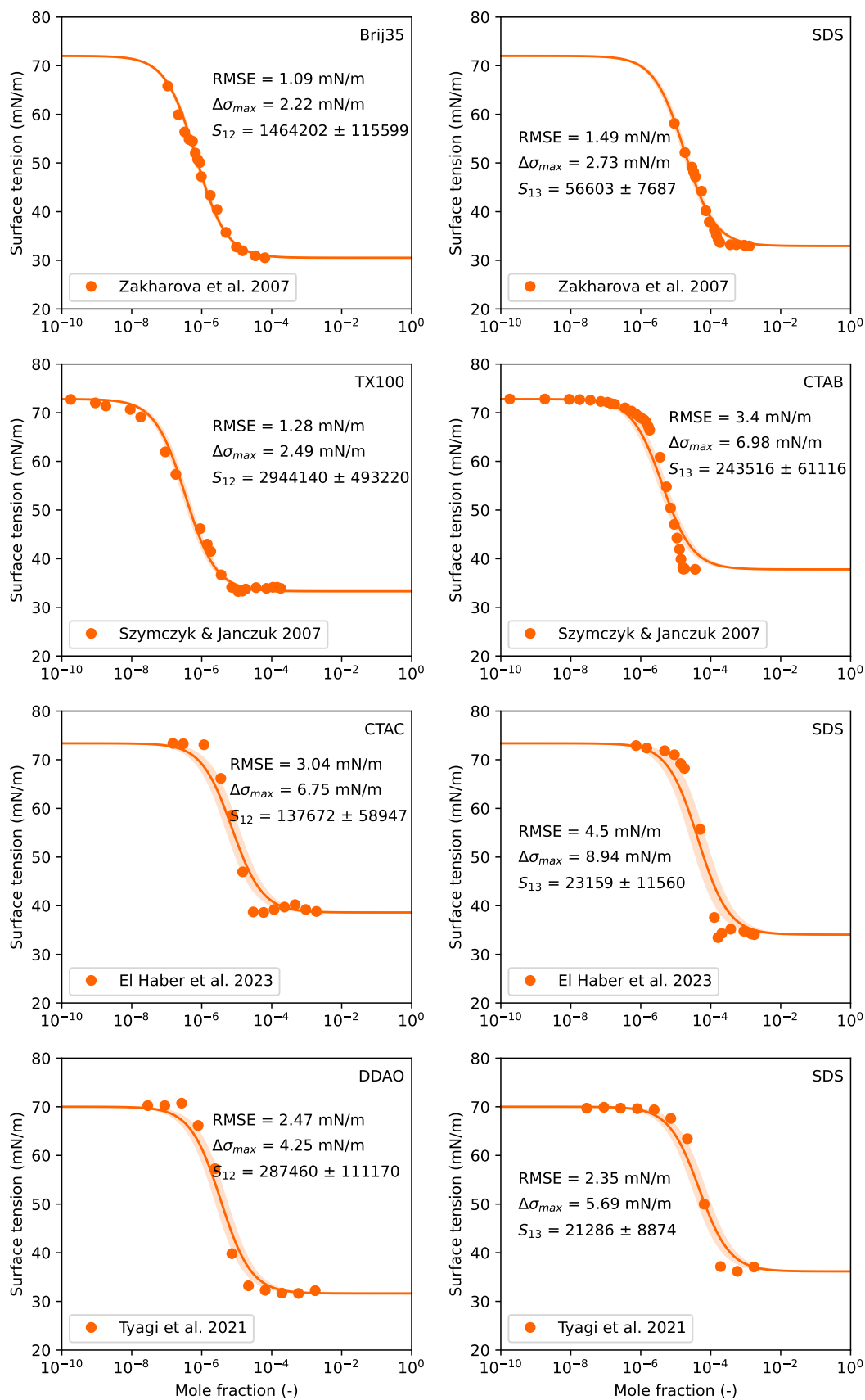## S5.2 Binary fits for water–surfactant–surfactant systems

Figure S7: Binary fits with the Eberhart model for the water–surfactant–surfactant systems. Light orange shading shows the 95% confidence interval.

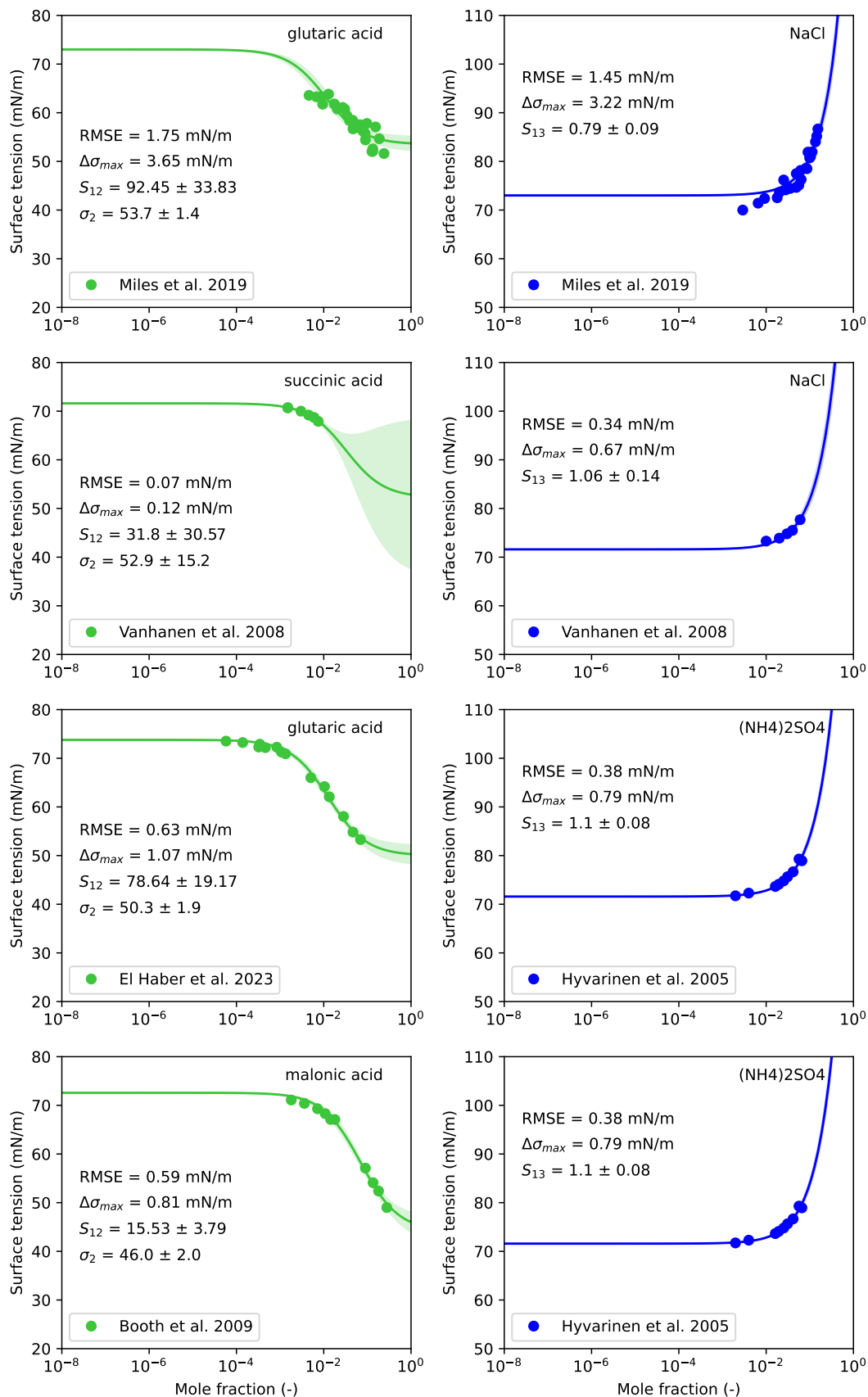## S5.3 Binary fits for water–organic–salt systems

Figure S8: Binary fits with the Eberhart model for the water–organic–salt systems. Light green and blue shading shows the 95% confidence interval.
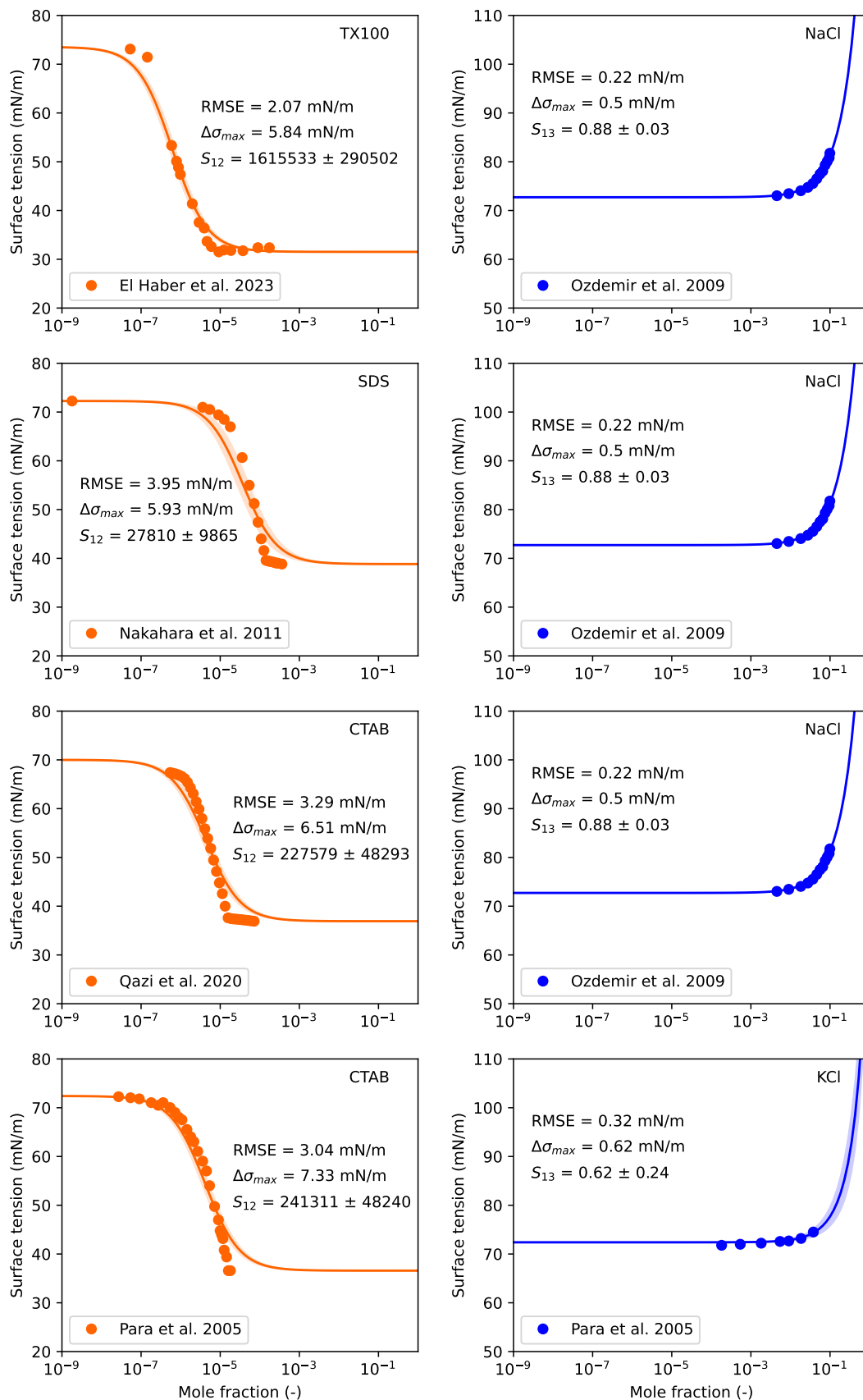
S5.4 Binary fits for water–surfactant–salt systems

Figure S9: Binary fits with the Eberhart model for the water–surfactant–salt systems. Light orange and blue shading shows the 95% confidence interval.

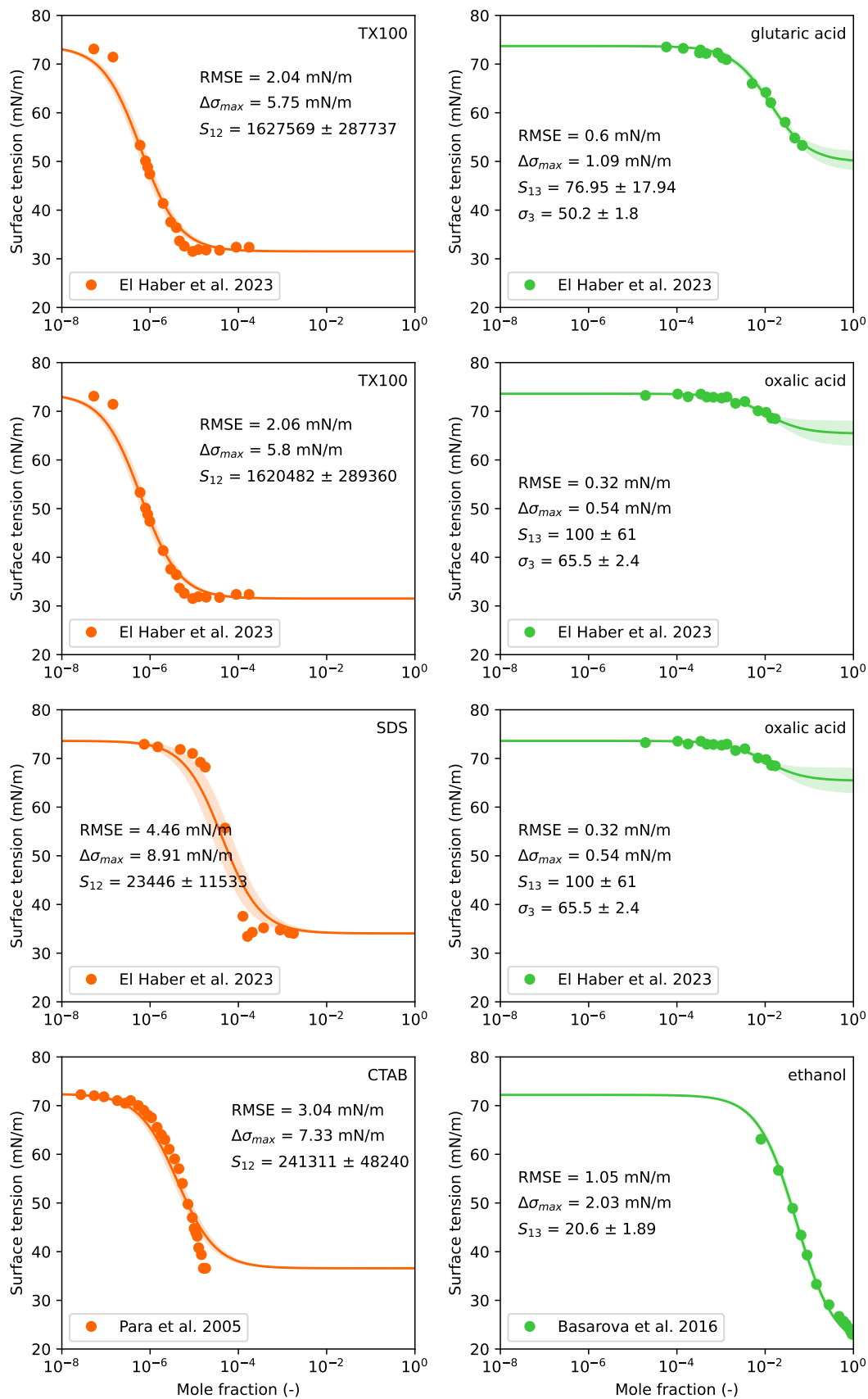## S5.5 Binary fits for water–surfactant–organic systems

Figure S10: Binary fits with the Eberhart model for the water–surfactant–organic systems. Light orange and green shading shows the 95% confidence interval.
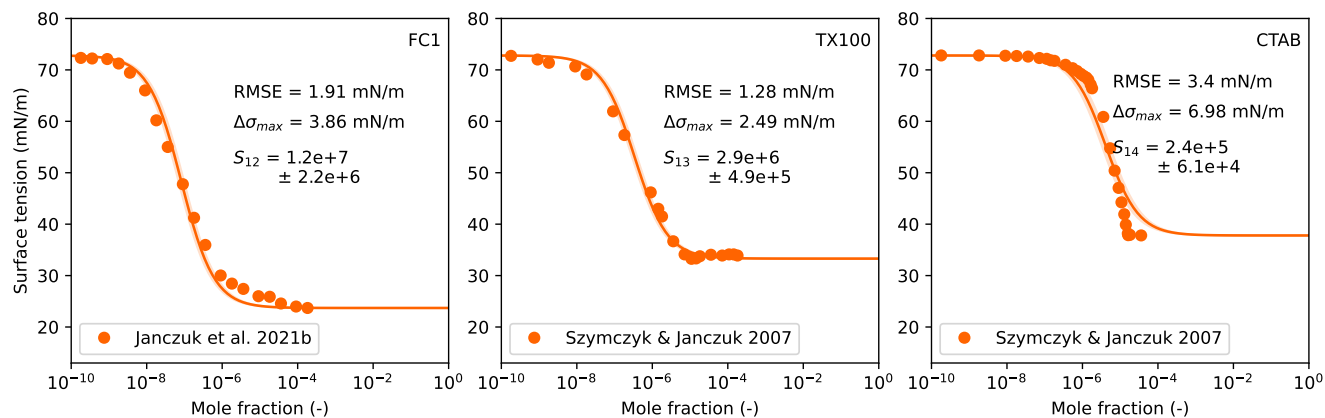
S5.6 Binary fits for a quaternary system

Figure S11: Binary fits with the Eberhart model for the quaternary system containing three surfactants. Light orange shading shows the 95% confidence interval.

S6 Additional tables and figures for ternary systems

S6.1 Ternary system properties tables

Table S10: Temperature (T), number of ternary datapoints (n_p), and measurement method of the ternary systems and the source data format. For data provided as figures in the original source, data was obtained with the help from digitisation software

System water (1) +	Reference	T °C	n_p	method	source
acetonitrile (2)+ 1,2-ethanediol (3)	50	25	52	du Noüy ring	table
n-butyl acetate (2)+ methanol (3)	51	30	48	du Noüy ring	table
Brij35 (2)+ SDS (3)	33	25	60	du Noüy ring	figure
TX100 (2)+ CTAB (3)	26	19	55	du Noüy ring	figure
CTAC (2)+ SDS (3)	18	24	41	pendant drop	table
DDAO (2)+ SDS (3)	32	25	53	pendant drop	figure
TX114 (2)+ SDS (3)	18	24	73	pendant drop	table
glutaric acid (2)+ NaCl (3)	75	25	30	microdroplet dispenser + optical tweezer	figure
succinic acid (2)+ NaCl (3)	82	25	16	capillary rise	table
glutaric acid (2)+ $(NH_4)_2SO_4$ (3)	18	24	22	pendant drop	table
malonic acid (2)+ $(NH_4)_2SO_4$ (3)	68	21	16	pendant drop	table
TX100 (2)+ NaCl (3)	18	24	60	pendant drop	table
SDS (2)+ NaCl (3)	62	25	100	drop volume method	figure
CTAB (2)+ NaCl (3)	64	21	453	du Noüy ring	table
CTAB (2)+ KCl (3)	63	21	149	pendant drop	figure
TX100 (2)+ $(NH_4)_2SO_4$ (3)	18	24	33	pendant drop	table
TX100 (2)+ glutaric acid (3)	18	24	101	pendant drop	table
TX100 (2)+ oxalic acid (3)	18	24	63	pendant drop	table
SDS (2)+ oxalic acid (3)	18	24	45	pendant drop	table
CTAB (2)+ ethanol (3)	53	19	243	du Noüy ring	figure
Brij35 (2)+ glutaric acid (3)	18	24	80	pendant drop	table

Table S11: Molar mass ($\tilde{M}$) and density (ρ) used for conversion of molar concentration or mass fraction to mole fractions for the ternary systems where needed

System water (1) +	$\tilde{M}_1$ g mol^{-1}	$\tilde{M}_2$ g mol^{-1}	$\tilde{M}_3$ g mol^{-1}	ρ_1 kg L^{-1}	ρ_2 kg L^{-1}	ρ_3 kg L^{-1}
glutaric acid (2)+ NaCl (3)		132.12	58.44			
succinic acid (2)+ NaCl (3)		118.09	58.44			
glutaric acid (2)+ $(NH_4)_2SO_4$ (3)	18.00	132.12	132.14	1.00	1.43	1.77
TX100 (2)+ NaCl (3)	18.00	625.00	58.44	1.00	1.06	2.16
SDS (2)+ NaCl (3)	18.00	288.38	58.44	1.00	1.01	2.16
CTAB (2)+ NaCl (3)	18.00	364.45	58.44	1.00	1.23	2.16
CTAB (2)+ KCl (3)	18.00	364.45	74.55	0.99	1.23	1.98
TX100 (2)+ $(NH_4)_2SO_4$ (3)	18.00	625.00	132.14	1.00	1.06	1.77
TX100 (2)+ glutaric acid (3)	18.00	625.00	132.12	1.00	1.06	1.43
TX100 (2)+ oxalic acid (3)	18.00	625.00	90.03	1.00	1.06	1.90
SDS (2)+ oxalic acid (3)	18.00	288.38	90.03	1.00	1.01	1.90
CTAB (2)+ ethanol (3)	18.00	364.45	46.07	1.00	1.23	0.79
Brij35 (2)+ glutaric acid (3)	18.00	1199.54	132.12	1.00	1.05	1.43
CTAC (2)+ oxalic acid (3)	18.00	320.00	90.03	1.00	0.97	1.90

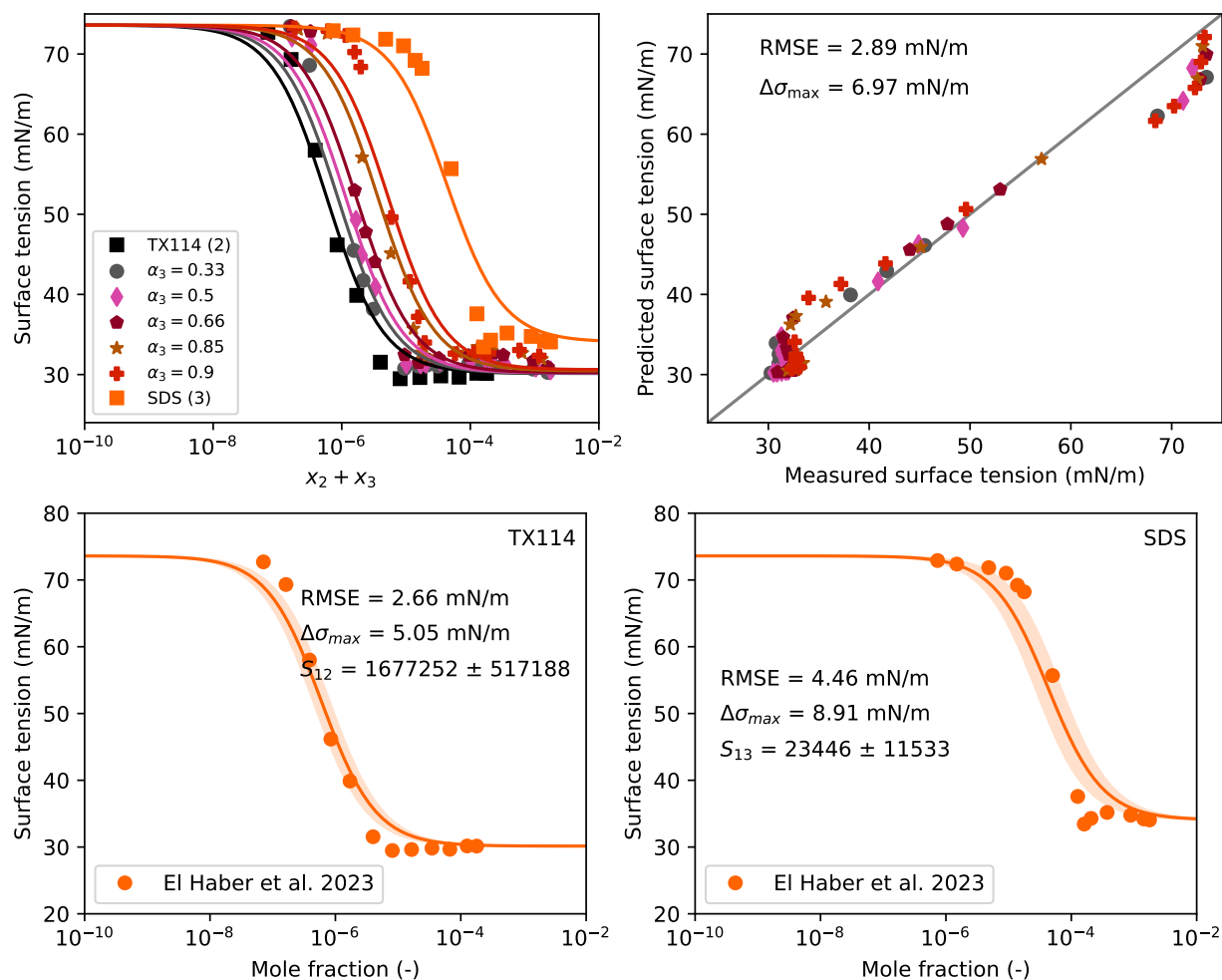## S6.2 Water–surfactant–surfactant

Figure S12: Surface tension of the system water (1) + TX114 (2) + SDS (3). The upper left panel shows experimental data from El Haber *et al.*[18] at $T = 24\,^{\circ}\mathrm{C}$ (symbols) and model results (solid lines) from Equations 4 and 8. The upper right panel shows the error in predicted surface tension for all ternary data points. The dry mole fraction α_3 is defined as $x_3/(x_2 + x_3)$. The lower panels show the binary water–surfactant fits. Light orange shading shows the 95% confidence interval.
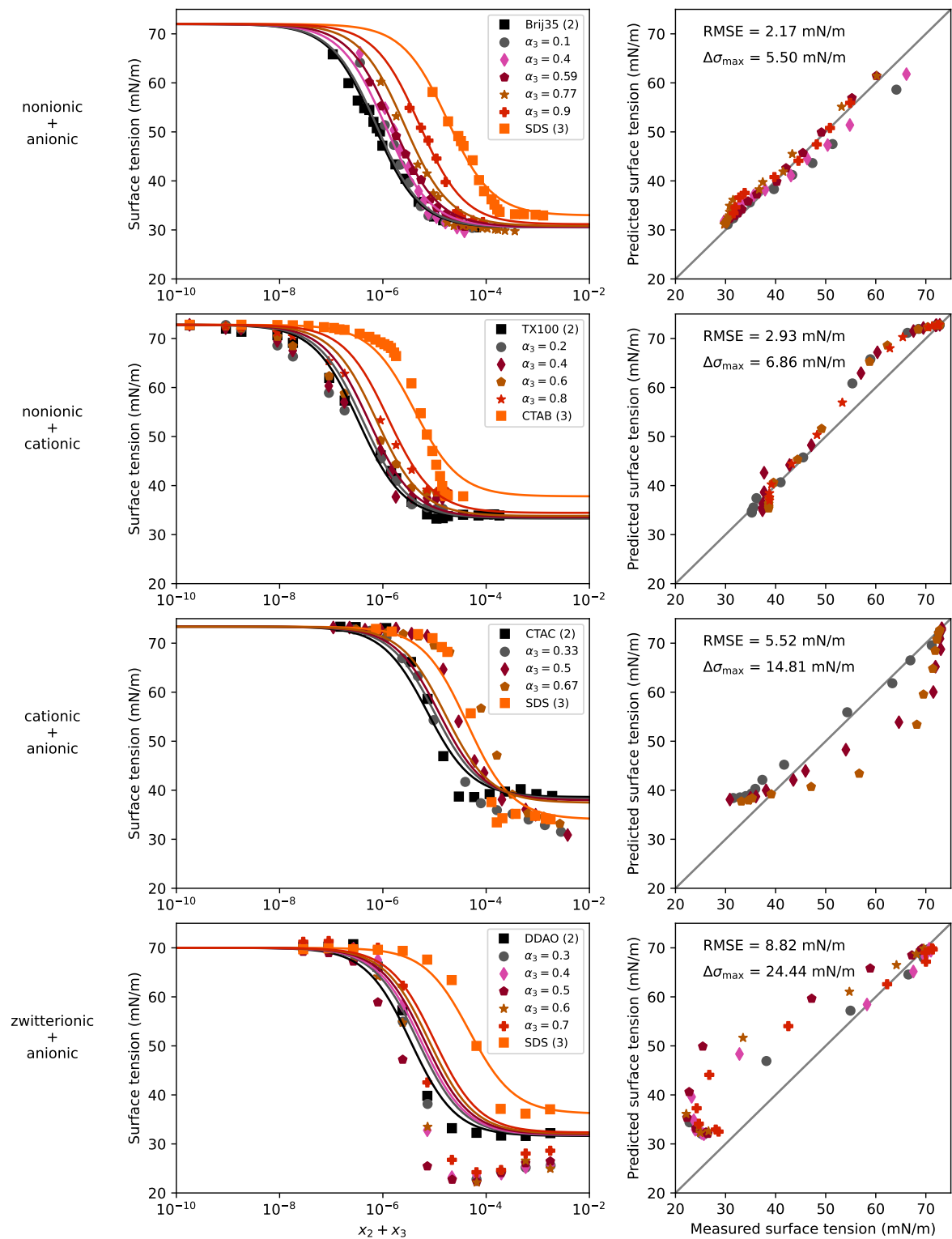
Figure S13: Same as Fig. 4 in the main paper but using the model in its fully predictive form (Equation 8, $A_{23} = 0$, $B_{23} = 0$, $S_{23} = 1$).

S6.3 Water–organic–salt

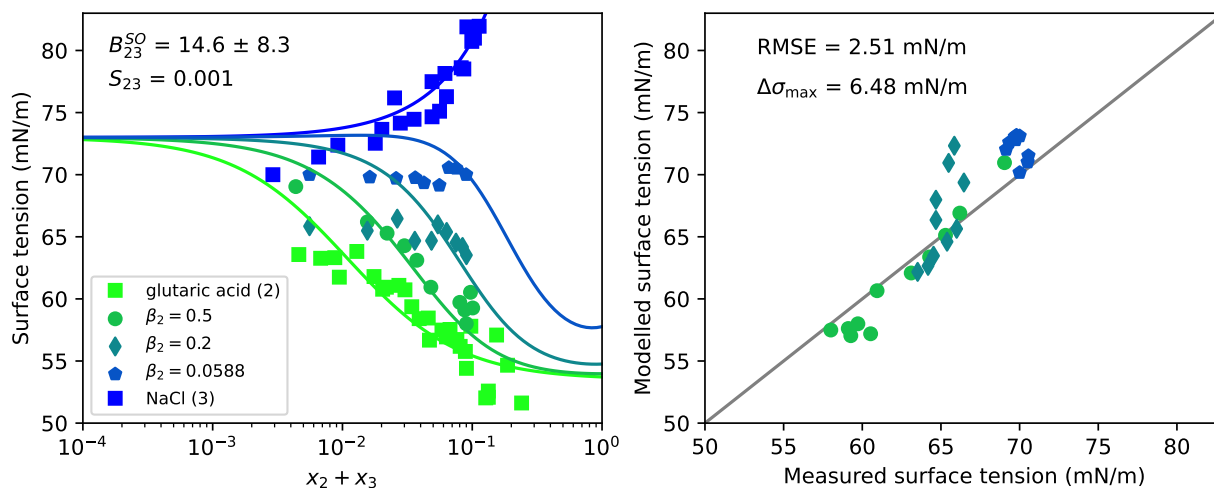Figure S14: Surface tension of the system water (1) + glutaric acid (2) + NaCl (3) with $S_{23} = 1 \times 10^{-3}$. The left panel shows experimental data from Miles *et al.*[75] at $T = 25\,^{\circ}\mathrm{C}$ (symbols) and model results (solid lines) from Equations 4, 8 and 9. The upper right panel shows the error in predicted surface tension for all ternary data points. The dry mass fraction β_2 is defined as $m_2/(m_2 + m_3)$ where m is the mass.
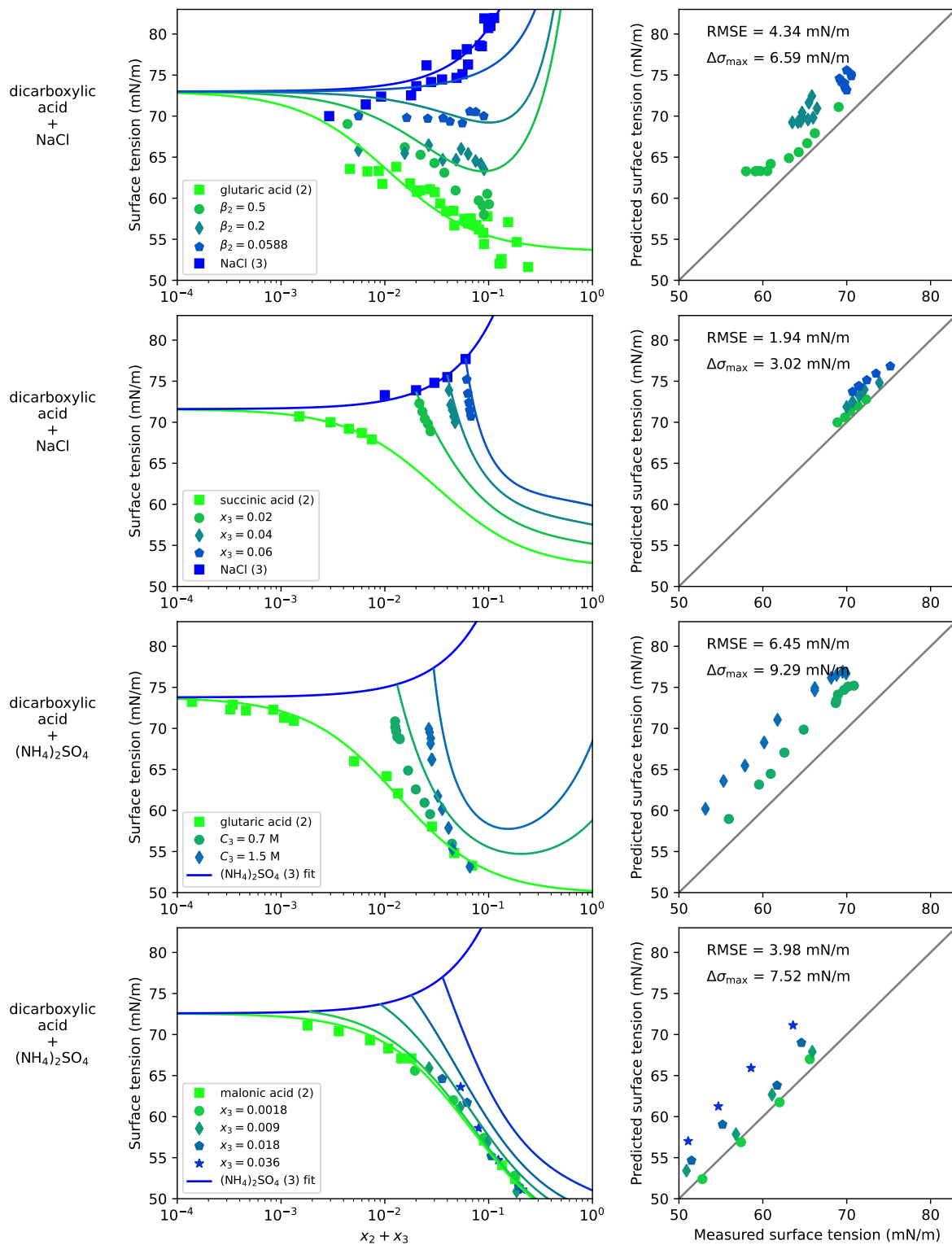
Figure S15: Same plot as Fig. 5 but without the salting-out factor ($F_{23} = 0$).
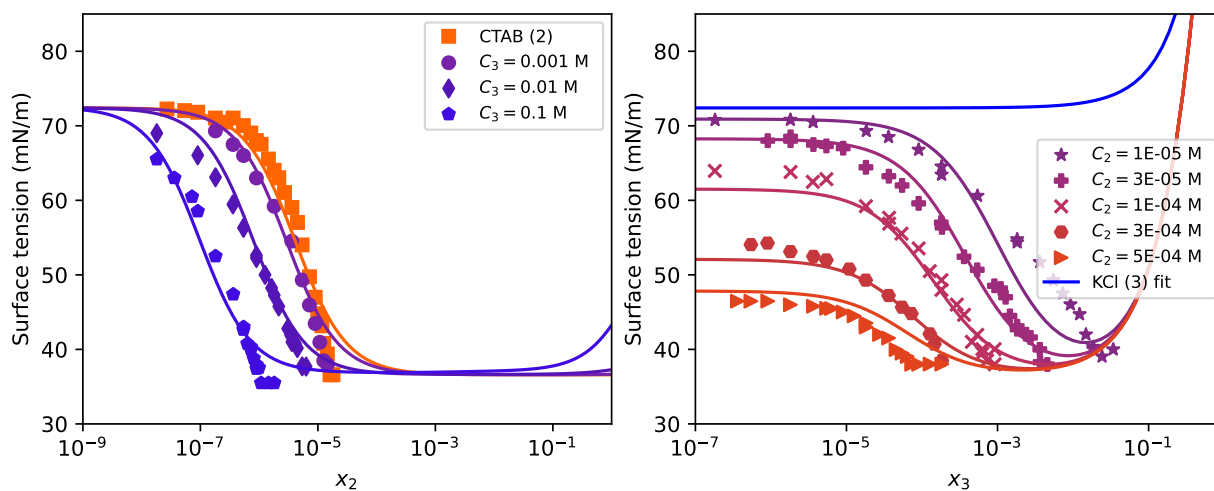
S6.4 Water–surfactant–salt

Figure S16: Surface tension of the system water (1) + CTAB (2) + KCl (3) shown on two different x-axes. Symbols show experimental data from Para *et al.* [63] at $T = 22\,^\circ$C and lines show model results from Equations 4, 8 and 9. C_i is the molar concentration of substance i in $\mathrm{mol\,L_{solution}^{-1}}$ (M).
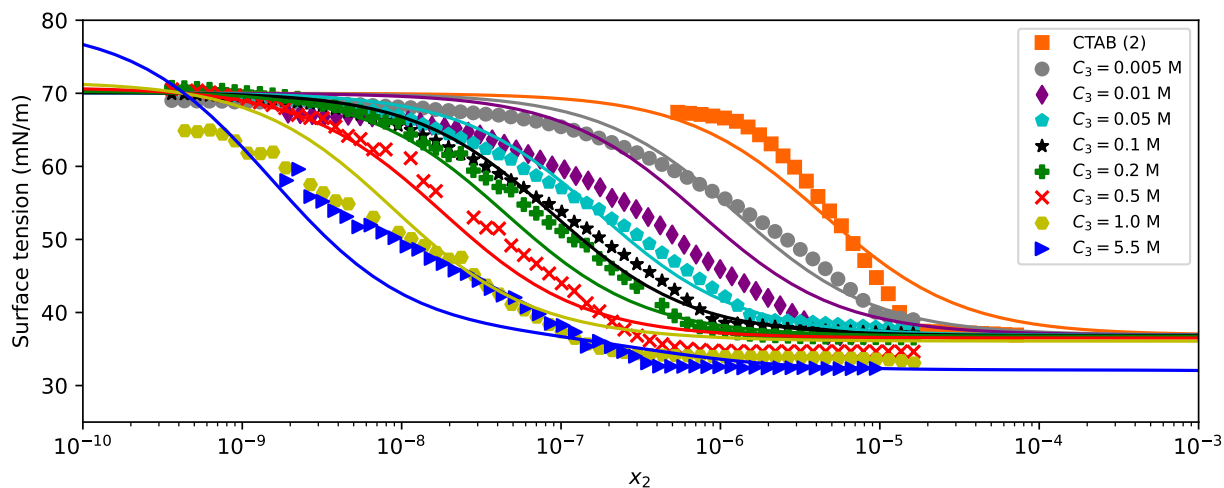

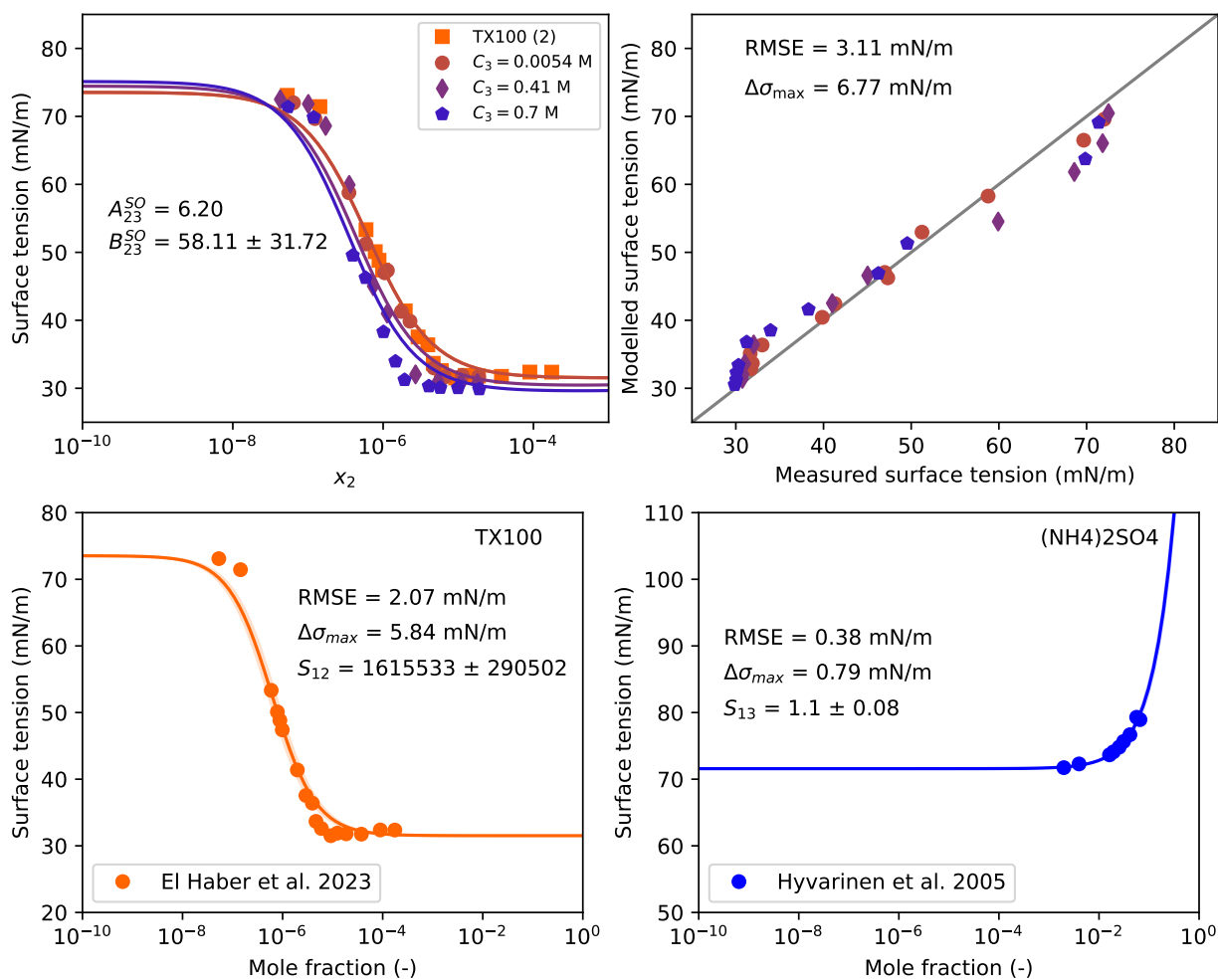Figure S17: Same plot as in the third panel of the left column in Fig. 6 with different colors.

Figure S18: Surface tension of the system water (1) + TX100 (2) + $(NH_4)_2SO_4$ (3). The upper left panel shows experimental data from El Haber *et al.*[18] at $T = 24\,°C$ (symbols) and model results (solid lines) from Equations 4, 8, and 9. The upper right panel shows the error in predicted surface tension for all ternary data points. C_3 is the molar concentration of substance (3) in $mol\,L_{solution}^{-1}$ (M). The lower panels show the binary water–surfactant fits. Light orange and blue shading shows the 95% confidence interval.
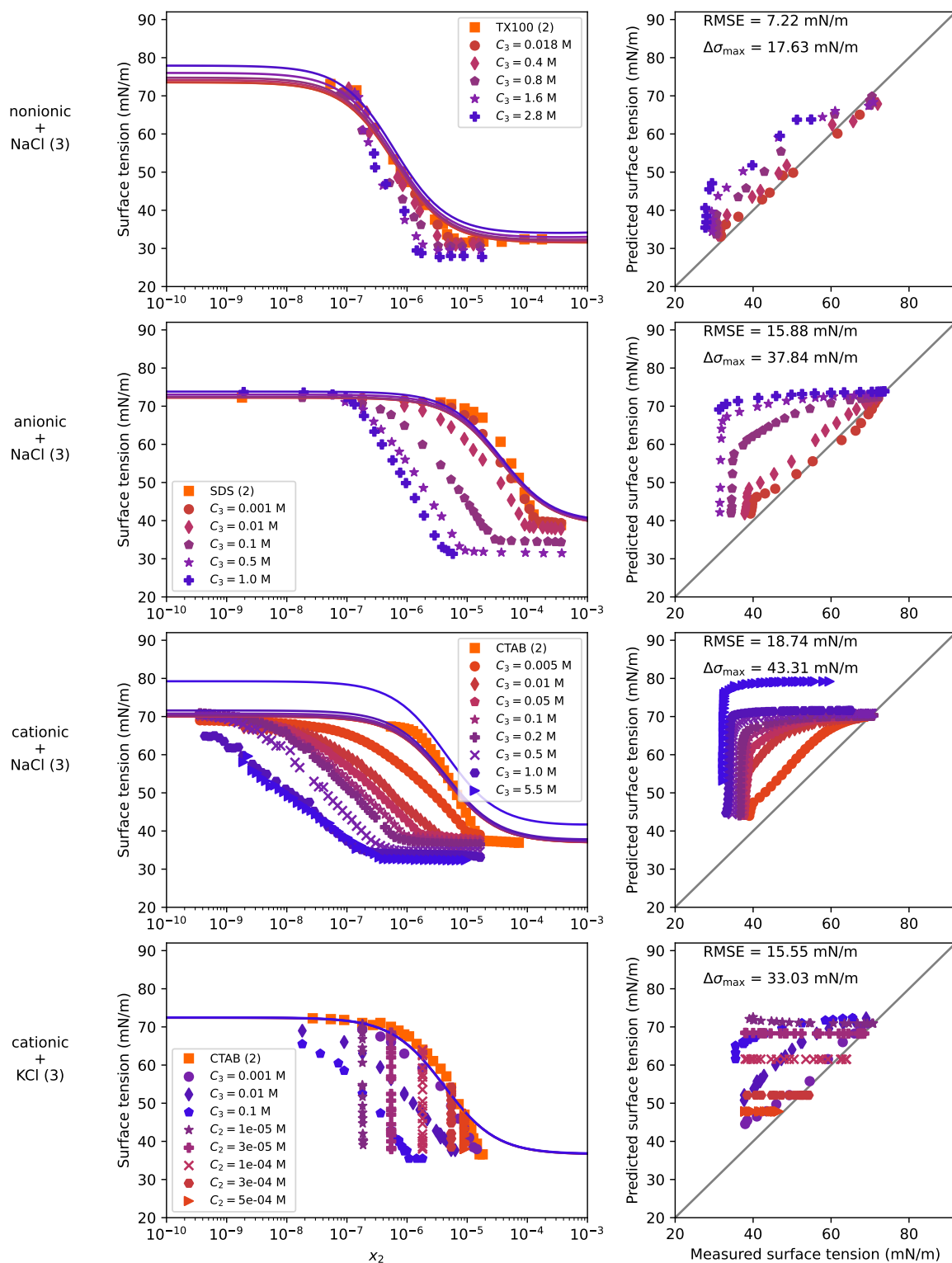
Figure S19: Same as Fig. 6 but using the model in its fully predictive form (Equation 8, $A_{23} = 0$, $B_{23} = 0$, $S_{23} = 1$).
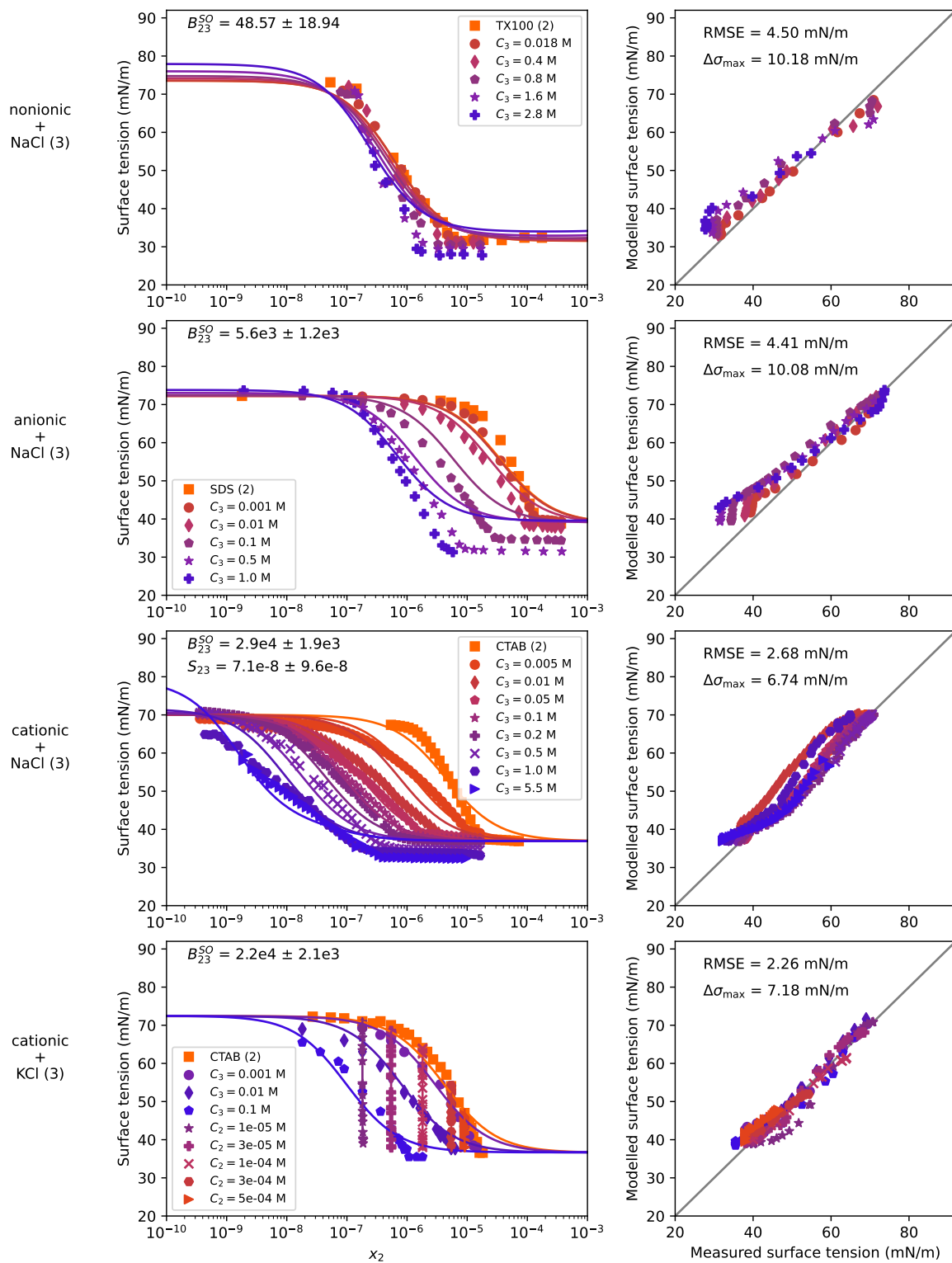
Figure S20: Same as Fig. 6 but without surface non-ideality ($A_{23} = 0$).

S6.5 Water–surfactant–organic
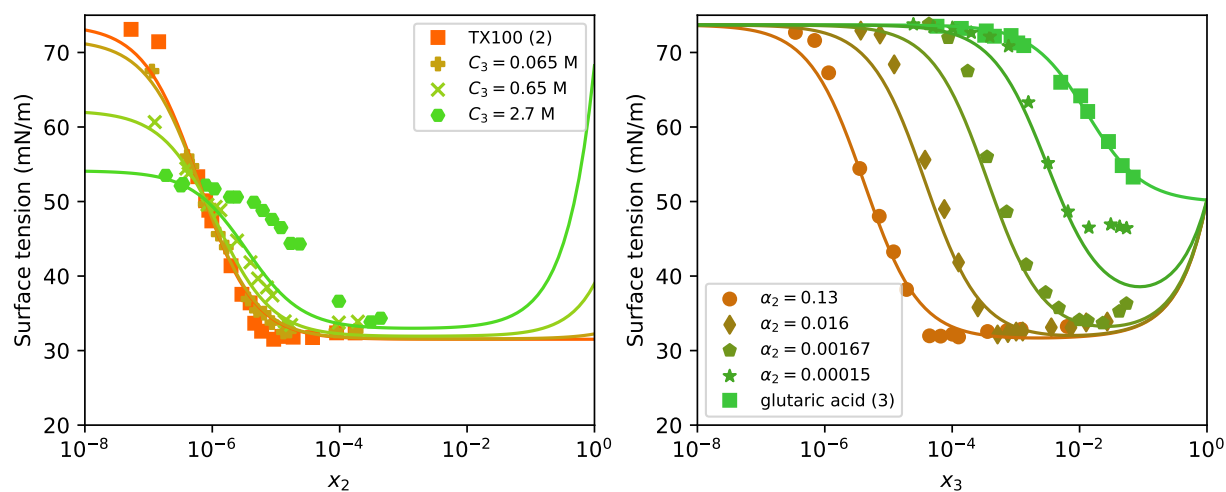
Figure S21: Surface tension of the system water (1) + TX100 (2) + glutaric acid (3) shown on two different x-axes. Symbols show experimental data from El Haber *et al.* [18] at $T = 24\,^\circ$C and lines show model results from Equations 4 and 8. The dry mole fraction α_2 is defined as $x_2/(x_2 + x_3)$. C_3 is the molar concentration of substance (3) in $\mathrm{mol\,L^{-1}_{solution}}$ (M).
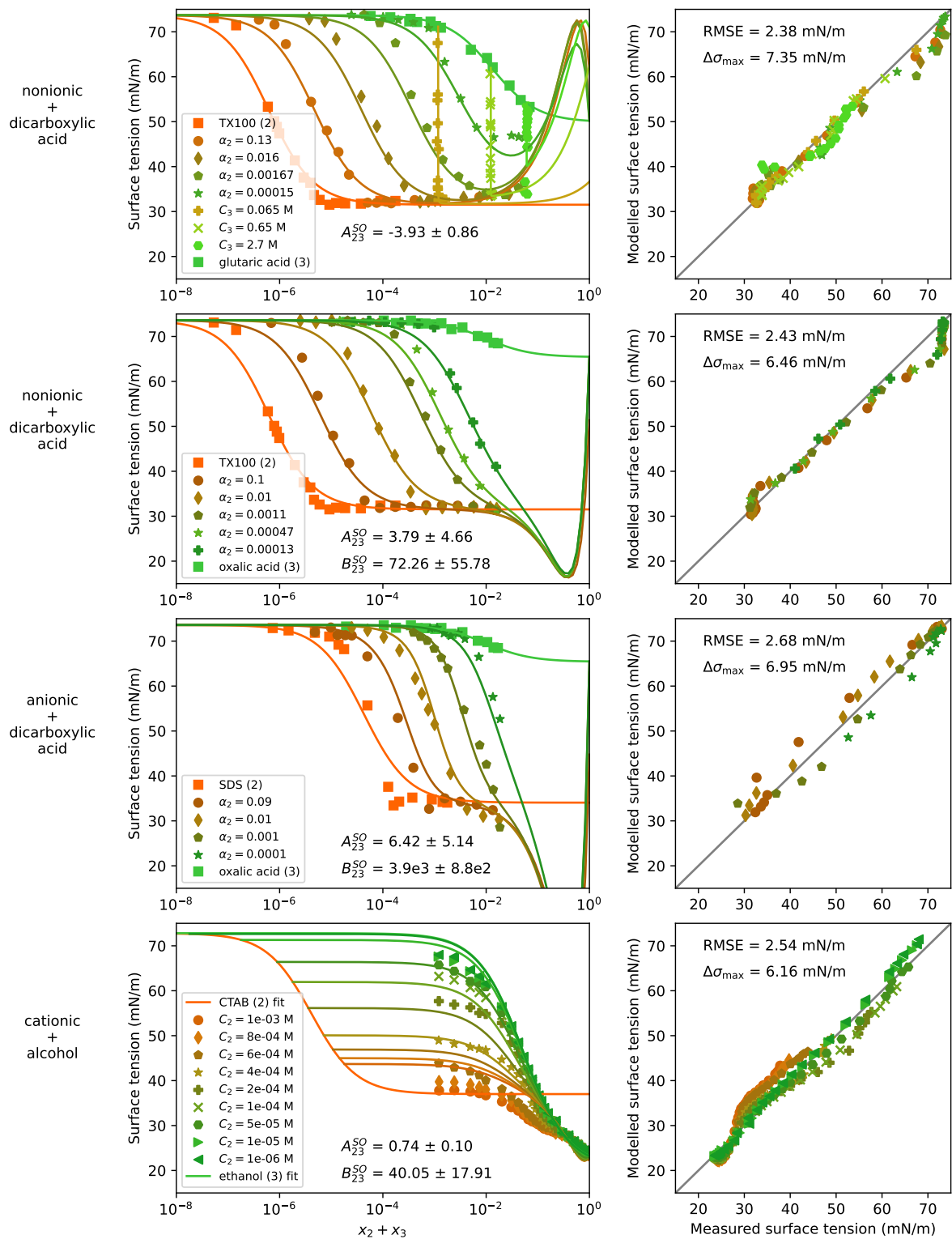
Figure S22: Same as Fig. 7 but with bulk and surface non-ideality effects included (Equations 9 and 10).
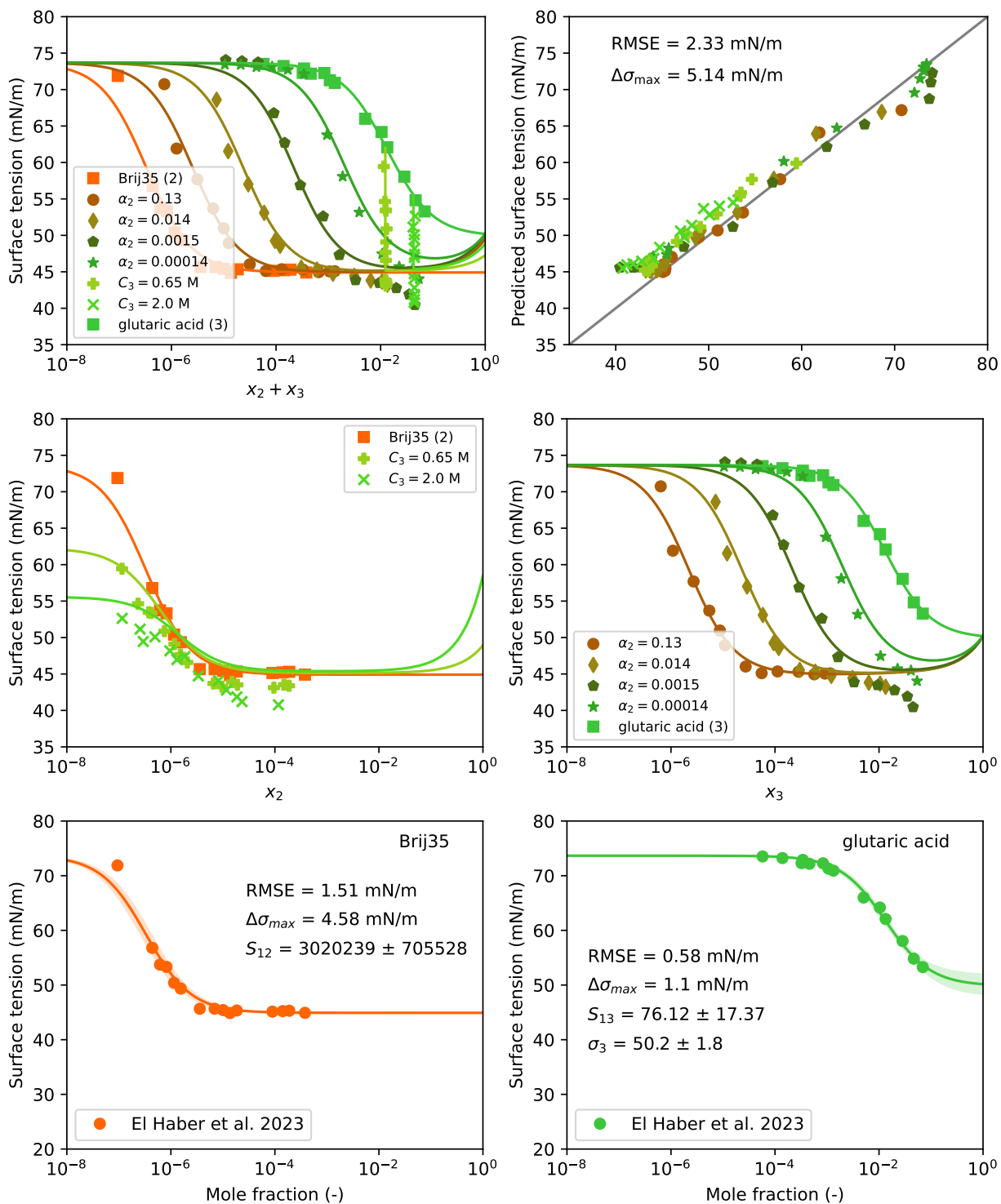
Figure S23: Surface tension of the system water (1) + Brij35 (2) + glutaric acid (3) shown on three different x-axes, the error in prediction (upper right panel) and the binary water–solute fits (lowest row). Symbols show experimental data from El Haber *et al.*[18] at $T = 24\,^{\circ}\text{C}$ and lines show model results from Equations 4 and 8. The dry mole fraction α_2 is defined as $x_2/(x_2 + x_3)$. C_3 is the molar concentration of substance (3) in $\text{mol}\,\text{L}_{\text{solution}}^{-1}$ (M).

Figure S24: Surface tension of the system water (1) + CTAC (2) + oxalic acid (3) and the binary water–solute fits (bottom row). Symbols show experimental data from El Haber *et al.* [18] at $T = 24\,°C$ and lines show model results from Equations 4, 8, 9, and 10. The dry mole fraction α_2 is defined as $x_2/(x_2 + x_3)$. C_3 is the molar concentration of substance (3) in $\mathrm{mol\,L_{solution}^{-1}}$ (M).

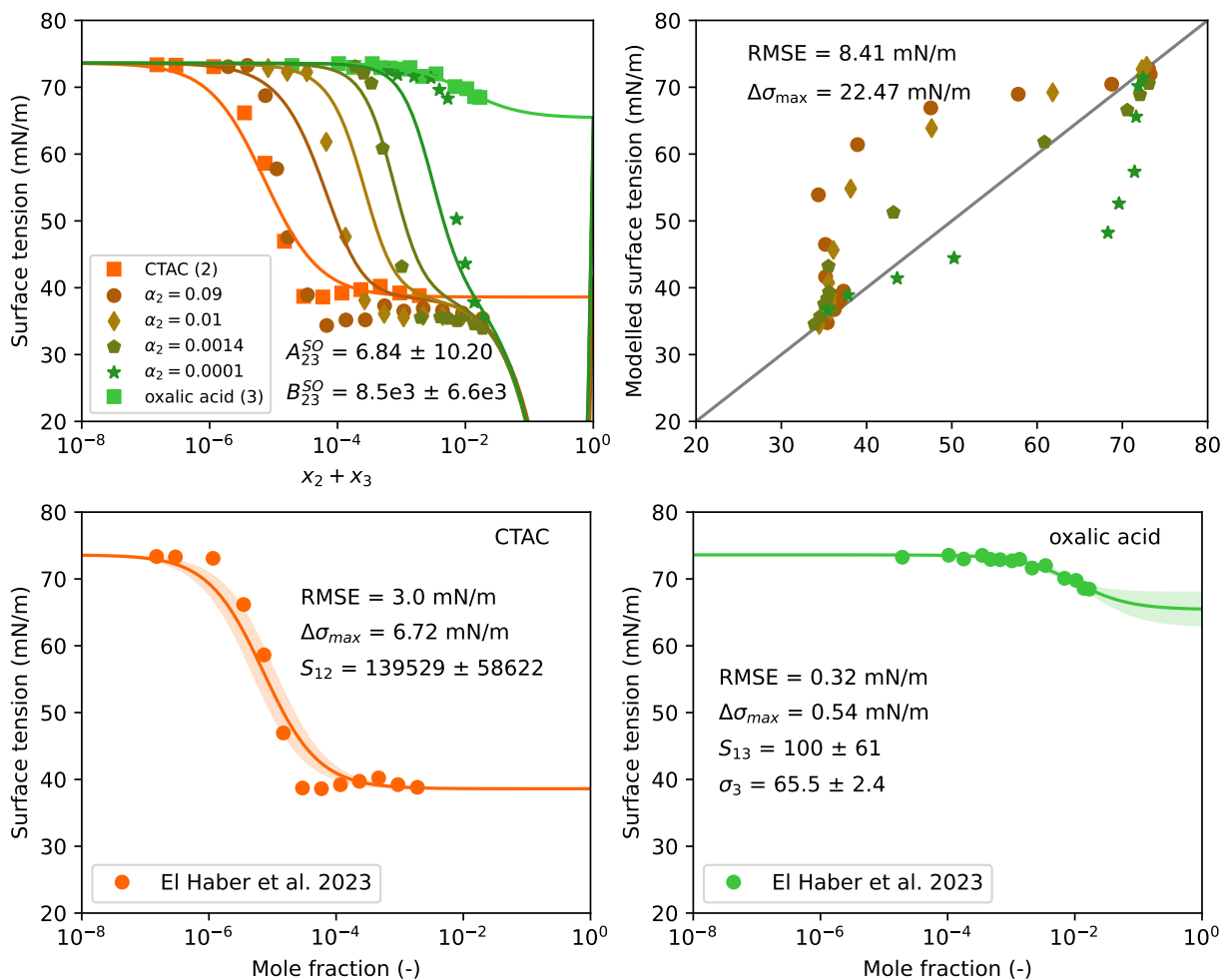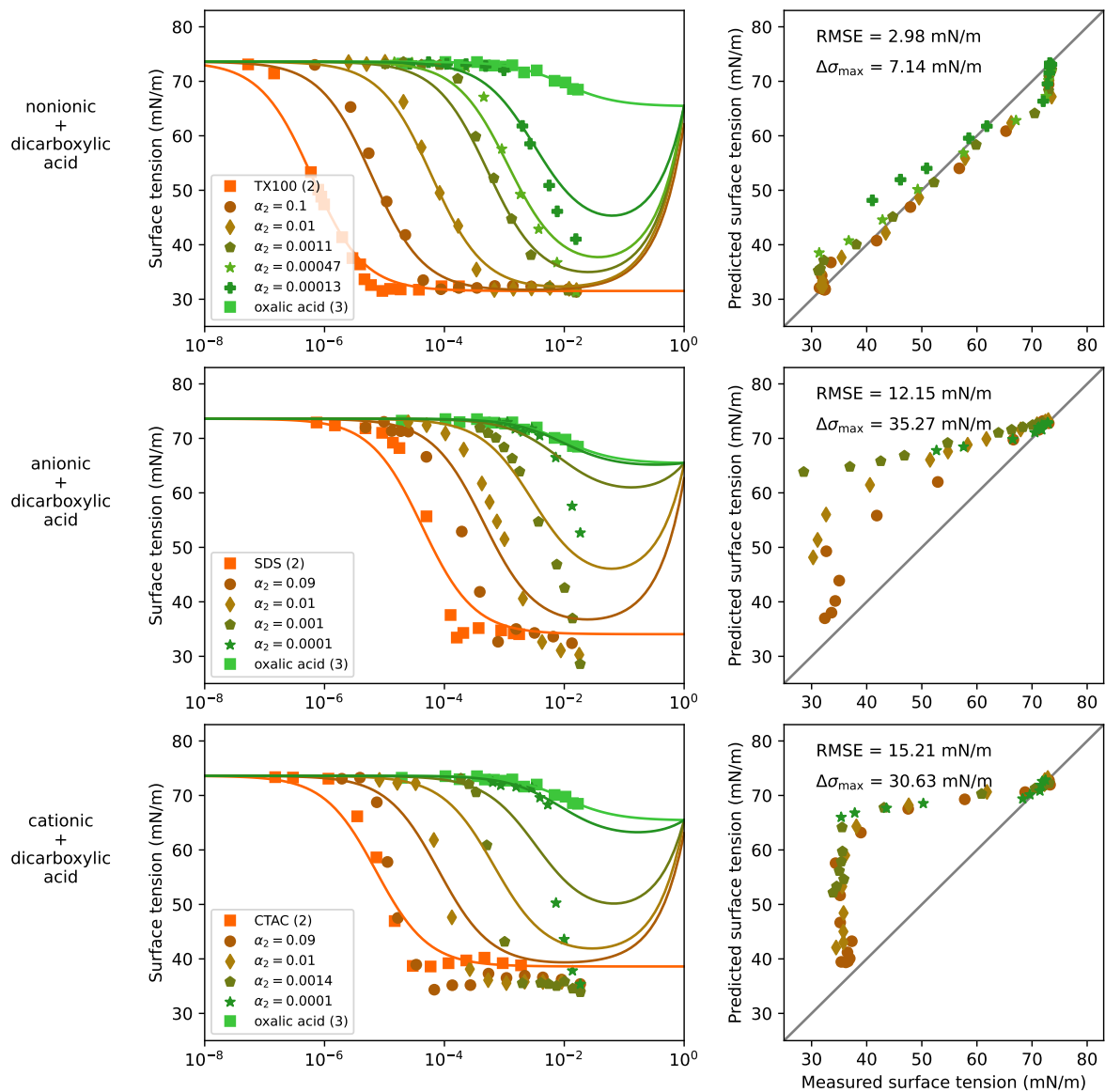Figure S25: Same as the second and third row in Fig. 7 and the first row in Fig. S24 but using the model in its fully predictive form (Equation 8, $A_{23} = 0$, $B_{23} = 0$, $S_{23} = 1$).

References

1 J. Kleinheins, N. Shardt, M. El Haber, C. Ferronato, B. Nozière, T. Peter and C. Marcolli, *Phys. Chem. Chem. Phys.*, 2023, **25**, 11055–11074.

2 K. A. Connors and J. L. Wright, *Analytical Chemistry*, 1989, **61**, 194–198.

3 N. Shardt, Y. Wang, Z. Jin and J. A. Elliott, *Chemical Engineering Science*, 2021, **230**, 116095.

4 L. Chunxi, W. Wenchuan and W. Zihao, *Fluid Phase Equilibria*, 2000, **175**, 185–196.

5 G. M. Wilson, *Journal of the American Chemical Society*, 1964, **86**, 127–130.

6 N. Shardt and J. A. W. Elliott, *Langmuir*, 2017, **33**, 11077–11085.

7 J. W. Belton, *Trans. Faraday Soc.*, 1935, **31**, 1413–1419.

8 J. W. Belton, *Trans. Faraday Soc.*, 1935, **31**, 1648–1652.

9 H. C. Boyer, B. R. Bzdek, J. P. Reid and C. S. Dutcher, *The Journal of Physical Chemistry A*, 2017, **121**, 198–205.

10 C. S. Dutcher, A. S. Wexler and S. L. Clegg, *The Journal of Physical Chemistry A*, 2010, **114**, 12216–12230.

11 A.-P. Hyvärinen, T. Raatikainen, A. Laaksonen, Y. Viisanen and H. Lihavainen, *Geophysical Research Letters*, 2005, **32**, L16806.

12 E. Martin, C. George and P. Mirabel, *Geophysical Research Letters*, 2000, **27**, 197–200.

13 N. Matubayasi, K. Tsunetomo, I. Sato, R. Akizuki, T. Morishita, A. Matuzawa and Y. Natsukari, *Journal of Colloid and Interface Science*, 2001, **243**, 444–456.

14 M. Nehma, J. M. Sangster and H. P. Schreiber, *Journal of Chemical & Engineering Data*, 1977, **22**, 156–158.

15 S. Alam, R. Ragupathy and A. B. Mandal, *Journal of Dispersion Science and Technology*, 2016, **37**, 1645–1654.

16 A. Bagheri and A. Abolhasani, *Korean Journal of Chemical Engineering*, 2015, **32**, 308–315.

17 C. Das, T. Chakraborty, S. Ghosh and B. Das, *Colloid Journal*, 2010, **72**, 788–798.

18 M. El Haber, C. Ferronato, A. Giroir-Fendler, L. Fine and B. Nozière, *Scientific Reports*, 2023, **13**, 20672.

19 V. Fainerman, R. Miller and E. Aksenenko, *Advances in Colloid and Interface Science*, 2002, **96**, 339–359.

20 N. Funasaki and S. Hada, *The Journal of Physical Chemistry*, 1979, **83**, 2471–2475.

21 B. Jańczuk, A. Zdziennicka, K. Szymczyk and M. L. González-Martín, *Colloids and Interfaces*, 2021, **5**, 53.

22 M. Mulqueen and D. Blankschtein, *Langmuir*, 1999, **15**, 8832–8848.

23 M. Mulqueen and D. Blankschtein, *Langmuir*, 2000, **16**, 7640–7654.

24 F. A. Siddiqui and E. I. Franses, *Langmuir*, 1996, **12**, 354–362.

25 K. Szymczyk, A. Zdziennicka, B. Jańczuk and W. Wójcik, *Colloids and Surfaces A: Physicochemical and Engineering Aspects*, 2005, **264**, 147–156.

26 K. Szymczyk and B. Jańczuk, *Colloids and Surfaces A: Physicochemical and Engineering Aspects*, 2007, **293**, 39–50.

27 K. Szymczyk and B. Jańczuk, *Langmuir*, 2007, **23**, 4972–4981.

28 K. Szymczyk and B. Jańczuk, *Langmuir*, 2010, **26**, 2491–2496.

29 K. Szymczyk, *Journal of Surfactants and Detergents*, 2011, **14**, 415–423.

30 K. Szymczyk, A. Zdziennicka, J. Krawczyk and B. Jańczuk, *The Journal of Chemical Thermodynamics*, 2014, **69**, 85–92.

31 A. Taraba and K. Szymczyk, *Annales Universitatis Mariae Curie-Sklodowska Chemistry Sectio AA*, 2017, **72**, 111–120.

32 G. Tyagi, D. Seddon, S. Khodaparast, W. N. Sharratt, E. S. Robles and J. T. Cabral, *Colloids and Surfaces A: Physicochemical and Engineering Aspects*, 2021, **618**, 126414.

33 L. Y. Zakharova, F. G. Valeeva, A. R. Ibragimova, V. M. Zakharov, L. A. Kudryavtseva, Y. G. Elistratova, A. R. Mustafina, A. I. Konovalov, S. N. Shtykov and I. V. Bogomolova, *Colloid Journal*, 2007, **69**, 718–725.

34 L.-H. Zhang and G.-X. Zhao, *Journal of Colloid and Interface Science*, 1989, **127**, 353–361.

35 L. Bartovská, M. Cechová, J. Matous and J. P. Novák, *Collection of Czechoslovak Chemical Communications*, 2000, **65**, 1487–1496.

36 P. Bošković, V. Sokol, T. Zemb, D. Touraud and W. Kunz, *The Journal of Physical Chemistry B*, 2015, **119**, 9933–9939.

37 H. F. Costa, H. Lourenço, I. Johnson, F. A. M. M. Gonçalves, A. G. M. Ferreira and I. M. A. Fonseca, *Journal of Chemical & Engineering Data*, 2009, **54**, 2845–2854.

38 R. S. Dzhambulatov, R. K. Dadashev, D. Z. Elimkhanov and I. N. Dadashev, *Russian Journal of Physical Chemistry A*, 2016, **90**, 1956–1959.

39 S. Enders, H. Kahl and J. Winkelmann, *Journal of Chemical & Engineering Data*, 2007, **52**, 1072–1079.

40 R. C. Ernst, C. H. Watkins and H. H. Ruwe, *The Journal of Physical Chemistry*, 1936, **40**, 627–635.

41 E. Golmaghani-Ebrahimi, A. Bagheri and M. Fazli, *Physics and Chemistry of Liquids*, 2018, **56**, 596–609.

42 D. Gómez-Díaz and J. M. Navaza, *Journal of Chemical & Engineering Data*, 2021, **66**, 2160–2166.

43 M. Hey and P. Kippax, *Colloids and Surfaces A: Physicochemical and Engineering Aspects*, 2005, **262**, 198–203.

44 I. Johnson, H. F. Costa, A. G. M. Ferreira and I. M. A. Fonseca, *International Journal of Thermophysics*, 2008, **29**, 619–633.

45 S. E. Kharin, A. Kniga and G. S. Sorokina, *Izvestiya Vysshikh Uchebnykh Zavedenii Khimiya iKhimicheskaya Tekhnologiya*, 1968, **12**, 1341–1344.

46 M. L. Kijevcanin, I. S. A. Ribeiro, A. G. M. Ferreira and I. M. A. Fonseca, *Journal of Chemical & Engineering Data*, 2003, **48**, 1266–1270.

47 M. Kijevcanin, I. Ribeiro, A. Ferreira and I. Fonseca, *Fluid Phase Equilibria*, 2004, **218**, 141–148.

48 S. Lamperski, *Journal of Colloid and Interface Science*, 1999, **213**, 360–370.

49 A. A. Rafati, A. Bagheri and M. Najafi, *Journal of Chemical & Engineering Data*, 2010, **55**, 4039–4043.

50 A. Rafati, A. Bagheri and M. Najafi, *The Journal of Chemical Thermodynamics*, 2011, **43**, 248–254.

51 B. Santos, A. Ferreira and I. Fonseca, *Fluid Phase Equilibria*, 2003, **208**, 1–21.

52 F. Beiranvand, S. H. Najibi and B. Hashemi Shahraki, *Iranian Journal of Oil and Gas Science and Technology*, 2020, **9**, 26–43.

53 M. Bielawska, A. Chodzińska, B. Jańczuk and A. Zdziennicka, *Colloids and Surfaces A: Physicochemical and Engineering Aspects*, 2013, **424**, 81–88.

54 B. R. Bzdek, J. P. Reid, J. Malila and N. L. Prisle, *Proceedings of the National Academy of Sciences*, 2020, **117**, 8335–8343.

55 S. Khosharay, M. Talebi, T. A. Saeed and S. S. Talaghani, *Journal of Molecular Liquids*, 2018, **249**, 245–253.

56 D. Kwaśniewska and J. Kiewlicz, *Journal of Saudi Chemical Society*, 2022, **26**, 101532.

57 D. Kwaśniewska and J. Kiewlicz, *Journal of Molecular Liquids*, 2022, **354**, 118917.

58 R. Wüstneck and R. Miller, *Colloids and Surfaces*, 1990, **47**, 15–21.

59 A. A. Dar, G. M. Rather, S. Ghosh and A. R. Das, *Journal of Colloid and Interface Science*, 2008, **322**, 572–581.

60 S. Helvaci, S. Peker and G. Özdemir, *Colloids and Surfaces B: Biointerfaces*, 2004, **35**, 225–233.

61 E. Matijević and B. A. Pethica, *Trans. Faraday Soc.*, 1958, **54**, 1382–1389.

62 H. Nakahara, O. Shibata and Y. Moroi, *The Journal of Physical Chemistry B*, 2011, **115**, 9077–9086.

63 G. Para, E. Jarek and P. Warszynski, *Colloids and Surfaces A: Physicochemical and Engineering Aspects*, 2005, **261**, 65–73.

64 M. J. Qazi, S. J. Schlegel, E. H. Backus, M. Bonn, D. Bonn and N. Shahidzadeh, *Langmuir*, 2020, **36**, 7956–7964.

65 J. P. Reid, B. J. Dennis-Smither, N.-O. A. Kwamena, R. E. H. Miles, K. L. Hanford and C. J. Homer, *Phys. Chem. Chem. Phys.*, 2011, **13**, 15559–15572.

66 M. C. K. Soule, P. G. Blower and G. L. Richmond, *The Journal of Physical Chemistry B*, 2007, **111**, 13703–13713.

67 J. W. Belton, *Trans. Faraday Soc.*, 1935, **31**, 1420–1425.

68 A. M. Booth, D. O. Topping, G. McFiggans and C. J. Percival, *Phys. Chem. Chem. Phys.*, 2009, **11**, 8021–8028.

69 S. Ekström, B. Nozière and H.-C. Hansson, *Atmospheric Chemistry and Physics*, 2009, **9**, 973–980.

70 M. Frosch, N. L. Prisle, M. Bilde, Z. Varga and G. Kiss, *Atmospheric Chemistry and Physics*, 2011, **11**, 3895–3911.

71 A.-P. Hyvärinen, H. Lihavainen, K. Hautio, T. Raatikainen, Y. Viisanen and A. Laaksonen, *Journal of Chemical & Engineering Data*, 2004, **49**, 917–922.

72 G. Kiss, E. Tombácz and H.-C. Hansson, *Journal of Atmospheric Chemistry*, 2005, **50**, 279–294.

73 H. D. Lee, A. D. Estillore, H. S. Morris, K. K. Ray, A. Alejandro, V. H. Grassian and A. V. Tivanski, *The Journal of Physical Chemistry A*, 2017, **121**, 8296–8305.

74 Z. Li, A. N. Schwier, N. Sareen and V. F. McNeill, *Atmospheric Chemistry and Physics*, 2011, **11**, 11617–11629.

75 R. Miles, M. Glerum, H. Boyer, J. Walker, C. Dutcher and B. Bzdek, *The Journal of Physical Chemistry A*, 2019, **123**, 3021–3029.

76 Y. Rublova, A. Kityk, F. Danilov and V. Protsenko, *Zeitschrift für Physikalische Chemie*, 2020, **234**, 399–413.

77 K. Sahu, V. F. McNeill and K. B. Eisenthal, *The Journal of Physical Chemistry C*, 2010, **114**, 18258–18262.

78 N. Sareen, A. N. Schwier, E. L. Shapiro, D. Mitroo and V. F. McNeill, *Atmospheric Chemistry and Physics*, 2010, **10**, 997–1016.

79 M. L. Shulman, M. C. Jacobson, R. J. Carlson, R. E. Synovec and T. E. Young, *Geophysical Research Letters*, 1996, **23**, 277–280.

80 D. O. Topping, G. B. McFiggans, G. Kiss, Z. Varga, M. C. Facchini, S. Decesari and M. Mircea, *Atmospheric Chemistry and Physics*, 2007, **7**, 2371–2398.

81 R. Tuckermann, *Atmospheric Environment*, 2007, **41**, 6265–6275.

82 J. Vanhanen, A.-P. Hyvärinen, T. Anttila, T. Raatikainen, Y. Viisanen and H. Lihavainen, *Atmospheric Chemistry and Physics*, 2008, **8**, 4595–4604.

83 J. Werner, M. Dalirian, M.-M. Walz, V. Ekholm, U. Wideqvist, S. Lowe, G. Ohrwall, I. Persson, I. Riipinen and O. Björneholm, *Environmental science & technology*, 2016, **50**, 7434–7442.

84 B. Svenningsson, J. Rissler, E. Swietlicki, M. Mircea, M. Bilde, M. C. Facchini, S. Decesari, S. Fuzzi, J. Zhou, J. Mønster and T. Rosenørn, *Atmospheric Chemistry and Physics*, 2006, **6**, 1937–1952.

85 L.-W. Chen, J.-H. Chen and N. F. Zhou, *J. Chem. Soc., Faraday Trans.*, 1995, **91**, 3873–3878.

86 B. Jańczuk, K. Szymczyk and A. Zdziennicka, *Molecules*, 2021, **26**, 4313.

87 K. Szymczyk, A. Zdziennicka and B. Jańczuk, *Journal of Molecular Liquids*, 2022, **345**, 117832.

88 S. Henning, T. Rosenørn, B. D'Anna, A. A. Gola, B. Svenningsson and M. Bilde, *Atmospheric Chemistry and Physics*, 2005, **5**, 575–582.

89 A. N. Schwier, N. Sareen, D. Mitroo, E. L. Shapiro and V. F. McNeill, *Environmental Science & Technology*, 2010, **44**, 6174–6182.

90 A. N. Schwier, G. A. Viglione, Z. Li and V. Faye McNeill, *Atmospheric Chemistry and Physics*, 2013, **13**, 10721–10732.

91 D. Góralczyk, K. Hac and P. Wydro, *Colloids and Surfaces A: Physicochemical and Engineering Aspects*, 2003, **220**, 55–60.

92 R. Tuckermann and H. K. Cammenga, *Atmospheric Environment*, 2004, **38**, 6135–6138.